

## **G.1 Methodology and Approach**

The approach and steps taken to assess potential impacts to the groundwater system are provided in this section. The alternatives considered in this assessment are described in detail in Section 3.3.

The analysis framework of this water quality assessment considers three major elements: source-term release, vadose zone transport, and groundwater transport. In addition, this analysis framework considers the eventual impact of predicted concentration levels in groundwater on the water quality of the Columbia River.

### **G.1.1 Lines of Analysis**

The lines of analysis (LOAs) used in this comparative assessment were located on the Hanford Site along lines approximately 1 km (0.6 mi) down-gradient of aggregate Hanford solid waste (HSW) disposal areas within the 200 East and West Areas, ERDF, and near the Columbia River located down-gradient from all disposal site areas (see Figure G.1). LOAs were selected based on transport results of unit releases at selected HSW disposal site locations. LOAs approximately 1 km (0.6 mi) down-gradient from the overall waste disposal facilities in each area are not meant to represent points of compliance, but rather common locations to facilitate comparison of impacts from broad waste management selections and locations defined for each alternative group.

Predicted constituent concentrations presented for each alternative group from specific water category releases represent maximum concentrations estimated along these LOAs. Because of the variation in the location of the different waste types and category releases for a given alternative group, the estimated maximum concentrations calculated from a specific waste category release may not correspond to the same point on the line analysis for every waste category and alternative group. For the sake of being conservative, however, combined concentration levels presented for each LOA and alternative group reflect the summation of predicted concentration levels regardless of their position on the LOA.

Delineation of waste impacts in the 200 East Area required two different LOAs. One LOA, designated as the 200 East Northwest (NW) LOA, is used to evaluate concentrations in groundwater migrating northwest of the 200 East Area. Another LOA, designated as the 200 East Southeast (SE) LOA, is used to evaluate concentrations in groundwater migrating southeast of the 200 East Area.

### **G.1.2 Overall Analysis Approach**

To estimate the concentration of contaminants in the groundwater, it was necessary to link the results of process models of waste release, transport through the vadose zone, and transport through the groundwater system. Two general approaches are available to link these models. One approach involves simulating a contaminant inventory distribution through each of the three process models. The other approach involves simulating a unit release through each of the three process models and superimposing these results with a specific constituent inventory distribution.

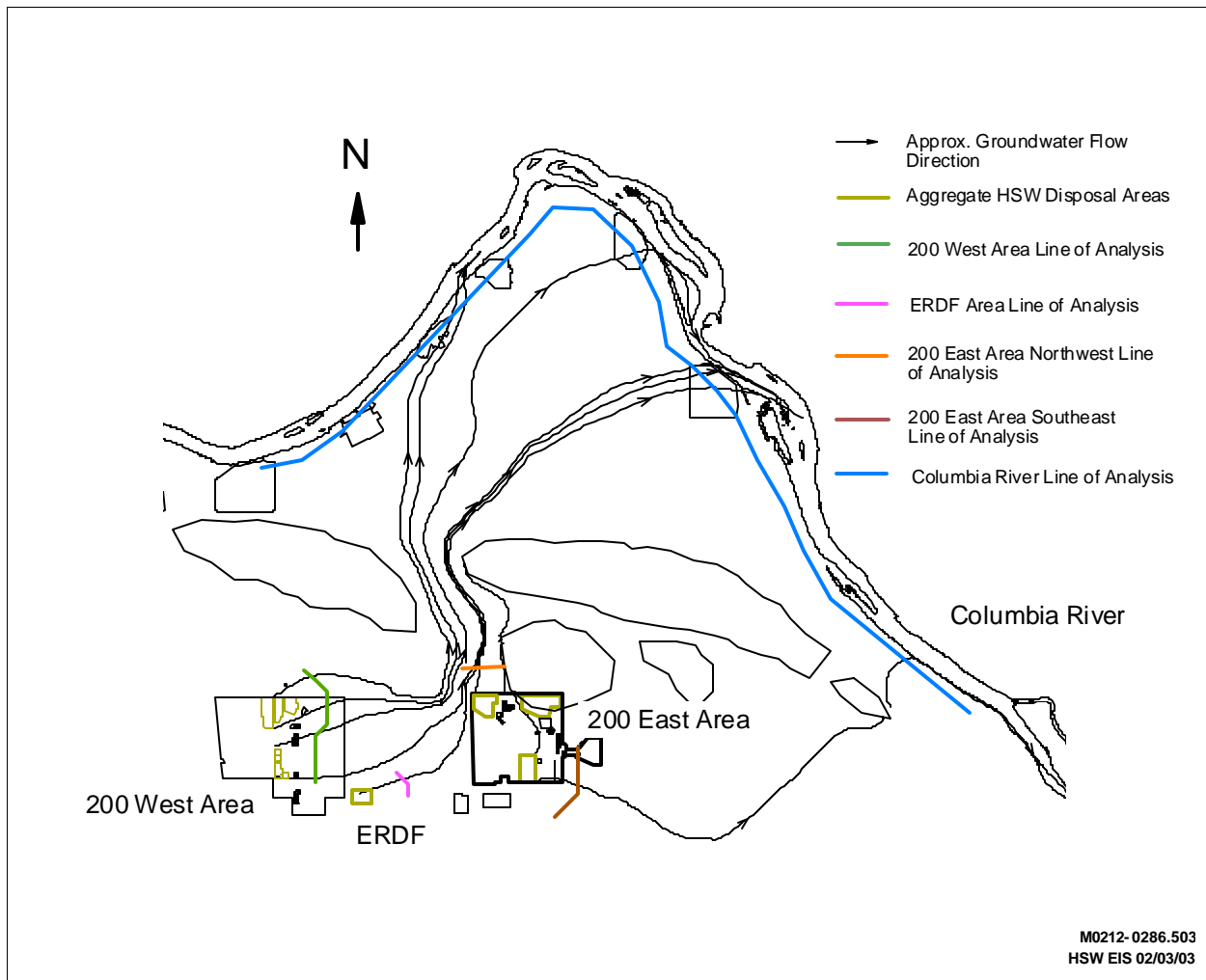


**Figure G.1.** Lines of Analysis Down-Gradient of Aggregate Hanford Solid Waste Disposal Areas

The first approach requires that each of the calculations be performed sequentially with each simulation representing a unique inventory distribution and parameter set. This approach is preferred when the number of combinations of inventory distributions and parameter sets is small compared to the total number of simulations required.

The second approach involves development of system output or response and, from that, a unit release that can be simulated for each source area, parameter set, and process model. (In this case, the process models include estimating source release, vadose zone flow and transport, and groundwater flow and transport.) Unit releases in each of the process models can be simulated independently. Then, by making the assumption of linearity, the unit release responses from each individual source area, via each of the process models, can be combined or superimposed using the convolution integral approach (Lee 1999). The convolution calculational approach is preferred when the number of combinations of inventory distributions and parameter sets is large, compared to the number of vadose zone and

1 groundwater flow and transport scenarios that need to be simulated. This second approach was selected  
2 for this analysis.

3  
4 The convolution approach and the implicit assumption of linearity provide a reasonable approach in  
5 approximating the long-term release of constituents from solid waste disposal facilities for the following  
6 reasons:

- 7  
8 • The waste zone environment of solid waste sources in HSW disposal facilities has been characterized  
9 as a low-organic, low salt, near neutral geochemical environment (Kincaid et al. 1998) and, as such,  
10 processes such as non-linear adsorption and other complex chemical reactions are not expected to  
11 have a substantial effect on contaminant release and transport through the vadose zone and  
12 groundwater water at the scales of interest (that is, down-gradient of the waste facilities to the  
13 Columbia River).
- 14  
15 • Wastes disposed of in HSW disposal facilities are largely dry solids and do not have any substantial  
16 amount of liquids or complex chemical fluids that could enhance migration of constituents to the  
17 underlying water table.
- 18  
19 • Waste releases are expected to occur over long periods of time and will likely reach the water table  
20 when the effect of past artificial discharges has dissipated and the unconfined aquifer returns to more  
21 natural conditions. Using estimates of infiltration through the vadose zone to the underlying  
22 groundwater that would reflect long-term average rates of natural recharge would appear reasonable.

23  
24 The convolution approach used also incorporates the process of solubility control that is assumed to  
25 be important in the source release for some constituents. The effect of this process is approximated by  
26 applying appropriate solubility controls in the source-term release component of the analysis. This  
27 approach can be effectively used without disrupting the superposition process. Solubility-controlled  
28 release models were used in the calculation of source-term release of the uranium isotopes in each of the  
29 alternatives.

30  
31 In the convolution integral calculational approach, the concentration in the groundwater at a specific  
32 location,  $i$ , at time,  $t$ , ( $C_{i,t}$ ) can be estimated using Equations G.1 and G.2:

$$33 \quad C_{i,t} = \sum_{s=1}^n M_s \sum_{T=1}^t (f_{s,T} c_{s,i,t-T+1}) \quad (G.1)$$

$$34 \quad f_{s,t} = \sum_{T=1}^t (r_{s,T} f_{s,t-T+1}) \quad (G.2)$$

35  
36  
37  
38 where  $C_{i,t}$  = Concentration at location,  $i$ , at time,  $t$

39  $M_s$  = Inventory at source,  $s$

1  $c_{s,i,t}$  = Groundwater concentration at  $i$  based on a unit release from  $s$  (Coupled Fluid, Energy,  
2 and Solute Transport [CFEST] model output)  
3  $r_{s,t}$  = Fractional release of unit inventory in source  $s$  at time  $t$  (Release model output)  
4  $f_{s,t}$  = Flux to water table from source,  $s$ , at time,  $t$ , based on unit release from  $s$  (Subsurface  
5 Transport Over Multiple Phases [STOMP] model output)  
6  $n$  = number of sources  
7 T = time integration variable.  
8

9 and where  $c_{s,i,t}$  and  $f_{s,t}$  are the discrete response functions estimated with the vadose zone and  
10 groundwater models based on a unit release. These discrete responses can be quickly combined with  
11 Equations G.1 and G.2 (that is, superimposed) in a variety of combinations to estimate system responses  
12 to different inventory distributions and parameter sets. (Note that equations G.1 and G.2 are discrete-  
13 approximation representations of the classic convolution integral calculational approach used in the  
14 calculation of superposition of responses in linear response systems.) The form of equation G.1 was also  
15 used to estimate the time-varying flux of a contaminant to the Columbia River by substituting the  
16 groundwater concentration based on a unit release from  $s$  with the calculated flux to the river based on a  
17 unit release from  $s$ . This river flux was combined with average annual river flows in the Columbia River  
18 to estimate river concentration levels that provided the basis for human health impacts and ecosystem risk  
19 from exposure to Columbia River water.  
20

21 Impacts from the subsurface transport pathway were analyzed for the LLBGs. The contaminant  
22 inventory for the LLBGs was released to the vadose zone according to an appropriate release model.  
23 Transport within the vadose zone was estimated with a steady-state, one-dimensional variably saturated  
24 vadose zone transport model by assuming a unit release for a range of recharge rates. Travel times for  
25 releases of unit mass were defined by arrival of 50 percent of each unit mass. These travel times were  
26 used to translate mass releases from the LLBGs into mass releases at the water table in the aquifer. The  
27 time-varying mass flux arriving at the water table reflects the entire time history of the mass release from  
28 the source area, as well as the calculated travel time in the vadose zone.  
29

30 Estimates of contaminant release transport from the LLBGs to the groundwater were evaluated. This  
31 evaluation was done by first calculating transport of 10-year releases of a unit of dry mass into the  
32 unconfined aquifer at the approximate locations of the LLBGs at the water table. These transport  
33 calculations were made with a steady-state, three-dimensional saturated groundwater flow and transient  
34 transport model. These calculated concentrations, based on a unit release, were then used in the  
35 convolution integral calculational method to translate transport of mass releases from the LLW through  
36 the vadose zone and the aquifer to specified locations down-gradient from the source areas. The  
37 concentrations in the groundwater plumes for each radionuclide were translated into doses using methods  
38 described in Appendix F.  
39

40 The sequence of calculations used in the long-term assessment required estimating the water quality  
41 impacts using a suite of process models that estimated source-term release, vadose zone flow and

transport, and groundwater flow and transport. The computational framework for these process models and relationship of software elements, which are schematically illustrated in Figure G.2, are as follows:

1. Excel™ workbook
2. Dynamically linked library version of the STOMP code (White and Oostrom 1996; White and Oostrom 1997; and Nichols et al. 1997)
3. Coupled Fluid Energy and Solute Transport (CFEST) code (Gupta 1997)

The concentrations in the groundwater plumes for each radionuclide were translated into human health impacts, which are summarized in Section 5.11 and Appendix F.

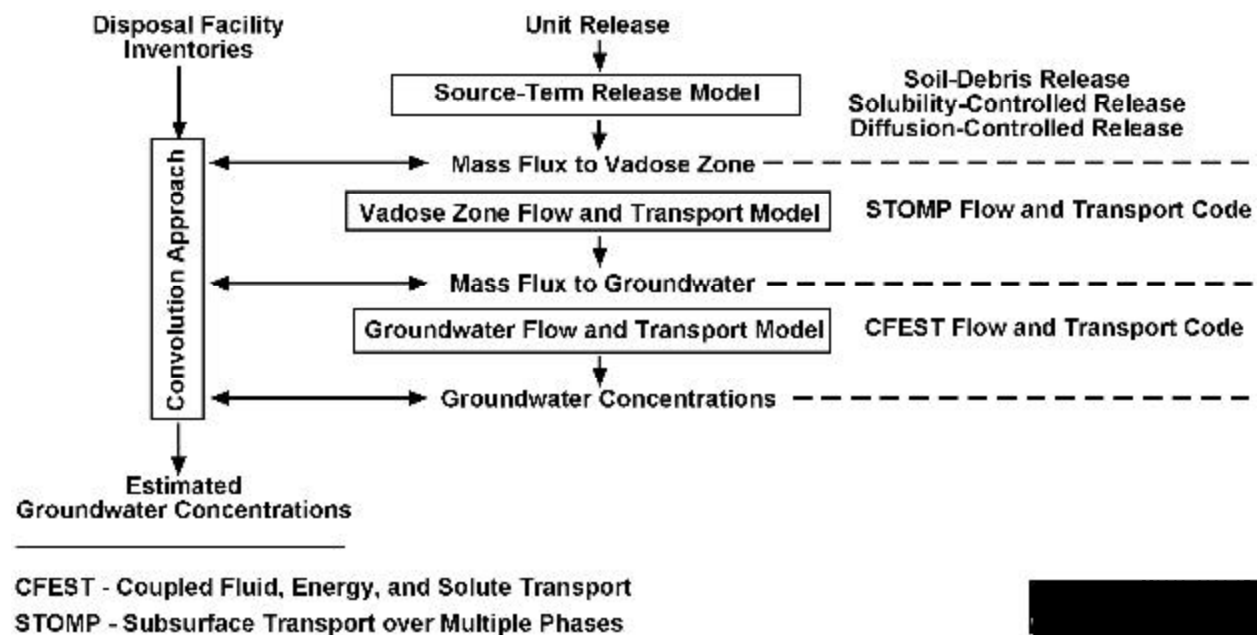


**Figure G.2.** Schematic Representation of Computational Framework and Codes Used in this HSW EIS

The methodologies for calculating source-term release, vadose zone transport, and groundwater transport are described in the following sections. Assumptions (for example, geometry, initial conditions, boundary conditions, and parameters) for each calculation are identified and discussed. The implementation of each model for each alternative is described.

### G.1.3 Source-Term Release

The source-term is the quantification of when and what constituents (by mass or activity) would be released. This source-term includes the water flux into the vadose zone that results from precipitation infiltrating the waste and mass or activity solubilized from dissolution of waste in the LLBGs. This section addresses the approach and methods used for source-term release that involve:

- 1 • Grouping of constituents into categories based on their mobility and screening to determine which  
2 constituents should be considered in this analysis  
3
- 4 • Aggregating potential sources into common source areas  
5
- 6 • Developing the contaminant inventories for each source area  
7
- 8 • Selecting appropriate source-term release models to calculate mass flux and fluid flux release as a  
9 function of time.  
10

### 11 **G.1.3.1 Constituent Grouping and Screening** 12

13 The LLBGs contain over 100 radioactive and non-radioactive constituents that potentially could  
14 impact groundwater. Screening of these constituents considered a number of aspects that included  
15 (1) their potential for dose or risk, (2) their estimated amount of inventory, and (3) their relative mobility  
16 in the subsurface system within a 10,000-year period of analysis.  
17

18 The assessment was the beneficiary of preceding analyses and field observations including the  
19 performance assessments for 200 West and 200 East post-1988 burial grounds (Wood et al. 1995, 1996),  
20 the remedial investigation and feasibility study of the ERDF (DOE 1994b), the disposal of ILAW  
21 originating from the single- and double-shell tanks (Mann et al. 1997) and (Mann et al. 2001), and the  
22 Composite Analysis of the 200 Area Plateau (Kincaid et al. 1998). These and other analyses, (for  
23 example, environmental impact statements) included development of inventory data and application of  
24 screening or significance criteria to identify those radionuclides that could be expected to substantially  
25 contribute to either the dose or risk calculated in the respective analysis. Clearly, those radionuclides  
26 identified as potentially significant in these published analyses are also expected to be key radionuclides  
27 in this assessment.  
28

29 To establish their relative mobility, the constituents were grouped based on their mobility in the  
30 vadose zone and underlying unconfined aquifer. Contaminant mobility classes were used rather than the  
31 individual mobility of each contaminant because of the uncertainty involved in determining the mobility  
32 of individual constituents. The mobility classes were selected based on relatively narrow ranges of  
33 mobility.  
34

35 Some of the constituents, such as iodine and technetium, would move at the rate of water whether in  
36 the vadose zone or underlying groundwater. The movement of other constituents in water, such as  
37 americium and cesium, would be slowed or retarded by the process of sorption onto soil and rock. A  
38 parameter that is commonly used to represent a measure of this sorption is referred to as the distribution  
39 coefficient or  $K_d$ . This parameter is defined as the ratio of the quantity of the solute adsorbed per gram of  
40 solid to the amount of solute remaining in solution (Kaplan et al. 1996). Values of  $K_d$  for the constituents  
41 range from 0 mL/g (in which the contaminant movement in water is not retarded) to more than 40 mL/g  
42 (in which the contaminant moves much slower than water).  
43

1 The LLW inventory constituents were grouped according to estimated or assumed  $K_d$  of each  
2 constituent. The constituent groups, based on mobility and examples of common constituents, are  
3 described in the following text. A summary of all constituents and associated groupings (based on  $K_d$   
4 values) is provided in Table G.1. The constituent classes used for modeling include:  
5

- 6 • **Mobility Class 1** – Contaminants were modeled as non-sorbing (that is,  $K_d = 0$ ) and would not be  
7 retarded in the soil-water system. Contaminant  $K_d$  values in this group ranged from 0 to 0.59 mL/g  
8 and include all the isotopes of iodine, technetium, selenium, chlorine, and tritium.  
9
- 10 • **Mobility Class 2** – Contaminants were modeled as slightly sorbing (that is,  $K_d = 0.6$ ) and would be  
11 slightly retarded in the soil-water system. Contaminant  $K_d$  values in this group ranged from 0.6 to  
12 0.99 mL/g and include all the isotopes of uranium and carbon.  
13
- 14 • **Mobility Class 3** – Contaminants were modeled as slightly more sorbing (that is,  $K_d = 1$ ).  
15 Contaminant  $K_d$  values in this group ranged from 1 to 9.9 mL/g and include all the isotopes of  
16 barium.  
17
- 18 • **Mobility Class 4** – Contaminants were modeled as moderately sorbing (that is,  $K_d = 10$ ).  
19 Contaminant  $K_d$  values in this group ranged from 10 to 39.9 mL/g and include all the isotopes of  
20 neptunium, palladium, protactinium, radium, and strontium.  
21
- 22 • **Mobility Class 5** – Contaminants were modeled as strongly sorbing (that is,  $K_d = 40$ ). Contaminant  
23  $K_d$  values in this group were 40 mL/g or greater and include all the isotopes of actinium, americium,  
24 cobalt, curium, cesium, iron, europium, gallium, niobium, nickel, lead, plutonium, samarium, tin,  
25 thorium, and zirconium.  
26

27 The constituent listing in Table G.1 was further evaluated using estimates of constituent transport  
28 times through the thick vadose zone to the unconfined aquifer during the 10,000-year period of analysis.  
29 For purposes of this analysis, the infiltration rate selected was 0.5 cm/yr. This rate was assumed, based  
30 on recharge estimates for different site surface conditions by Fayer et al. (1999), to reflect a conservative  
31 estimate of infiltration for surface conditions that would be expected to persist at the LLBGs during the  
32 post-closure period. Estimates by Fayer et al. (1999) indicate that infiltration rates for surface conditions  
33 that have a modified Resource Conservation and Recovery Act (RCRA) Subtitle C cover system would  
34 be below the assumed 0.5 cm/yr rate used in this screening analysis.  
35

36 Based on this assumed infiltration rate and estimated levels of sorption and associated retardation for  
37 each of the classes above, estimated travel times of all constituents in Mobility Classes 3, 4, and 5 through  
38 the thick vadose zone to the unconfined aquifer beneath the LLBGs were calculated to be well beyond the  
39 10,000-year period of analysis. Thus, all constituents in these classes were eliminated from further  
40 consideration.

1  
2

**Table G.1.** Constituents Categorized by Mobility ( $K_d$ ) Classes

<b>Mobility Class 1 (<math>K_d = 0.0</math> mL/g)</b>				
<b>Constituent</b>	<b>Best <math>K_d</math> Estimate</b>	<b>Range of <math>K_d</math> Estimates</b>	<b>Reference</b>	<b>Half-Life (years)</b>
H-3	0	0 – 0.5	Kincaid <i>et al.</i> (1998)	1.2E+01
Tc-99	0	0 – 0.6 0 – 0.1	Kincaid <i>et al.</i> (1998) Cantrell <i>et al.</i> (2002)	2.1E+05
I-129	0.3	0.2 – 15 0 – 2	Kincaid <i>et al.</i> (1998) Cantrell <i>et al.</i> (2002)	1.5E+07
Cl-36	0	0-0.6	Kincaid <i>et al.</i> (1998)	3.8E+05
Se-79	0	0 – 0.78	Kincaid <i>et al.</i> (1998)	6.5E+05
<b>Mobility Class 2 (<math>K_d = 0.6</math> mL/g)</b>				
C-14	0.5	0.5 – 1000	Kincaid <i>et al.</i> (1998)	5.7E+03
U-232	0.6	0.1 – 79.9 0.2 - 4	Kincaid <i>et al.</i> (1998)	6.9E+01
U-233			Cantrell <i>et al.</i> (2002)	1.5E+05
U-234				2.4E+05
U-235				7.0E+08
U-236				2.3E+07
U-238				4.5E+09
<b>Mobility Class 3 (<math>K_d = 1.0</math> mL/g)</b>				
Ba-133	1	N/A	Wood <i>et al.</i> (1995)	1.0E+01
<b>Mobility Class 4 (<math>K_d = 10.0</math> mL/g)</b>				
Np-237	15	2.4-21.9	Kincaid <i>et al.</i> (1998)	2.1E+06
Pa-231	15	2.4 – 21.9	Kincaid <i>et al.</i> (1998)	3.3E+04
Pd-107	10	N/A	DOE and Ecology (1996)	6.5E+06
Ra-226	20	5 – 173	Kincaid <i>et al.</i> (1998)	1.6E+03
Sr-90	20	5 – 173	Kincaid <i>et al.</i> (1998)	2.8E+01
		10 - 20	Cantrell <i>et al.</i> (2002)	
<b>Mobility Class 5 (<math>K_d = 40.0</math> mL/g)</b>				
Ac-227	300	67 – 1330	Kincaid <i>et al.</i> (1998)	2.1E.01
Am-241	300	67 – 1330	Kincaid <i>et al.</i> (1998)	4.3E+02
Am-242m				1.5E+02
Am-243				7.4E+03
Co-60	1200	1200 – 12500	Kincaid <i>et al.</i> (1998)	5.3E+00
Cm-243	300	67 – 1330	Kincaid <i>et al.</i> (1998)	2.9E+01
Cm-244				1.8E+01
Cm-245				8.4E+03
Cm-246				4.7E+03
Cm-248				3.4E+05
Cs-135	1500	540 – 3180	Kincaid <i>et al.</i> (1998)	2.30E+06
Cs-137				3.0E+ 01
Eu-152	300	67 – 1330	Kincaid <i>et al.</i> (1998)	1.3E+01
Gd-152	100	N/A	Wood <i>et al.</i> (1996)	1.1E+14
Nb-94	300	50 – 2350	Kincaid <i>et al.</i> (1998)	2.0E+04
Ni-63	300	50 – 2350	Kincaid <i>et al.</i> (1998)	1.0E+02

Table G.1. (contd)

Constituent	Best $K_d$ Estimate	Range of $K_d$ Estimates	Reference	Half Life (years)
<b>Mobility Class 5 (<math>K_d = 40.0</math> mL/g) - continued</b>				
Pb-210	2000	13000 – 79000	Kincaid <i>et al.</i> (1998)	2.2E+01
Pu-238	200	80 – >1980	Kincaid <i>et al.</i> (1998)	8.7E+01
Pu-229				2.4E+04
Pu-240				6.5E+03
Pu-242				3.7E+05
Pu-244				8.1E+07
Th-229	1000	40 – >2000	Kincaid <i>et al.</i> (1998)	7.3E+03
Th-230				7.7E+04
Th-232				1.4E+10
Sm-147	100	N/A	Wood <i>et al.</i> (1996)	1.1E+11
Sn-126	50	50 – 2350	Kincaid <i>et al.</i> (1998)	9.9E+04
Zr-93	1000	40 – >2000	Kincaid <i>et al.</i> (1998)	1.5E+06
N/A – Not applicable.				

Of the suite of remaining waste constituents, technetium-99 and iodine-129 in Mobility Class 1 and carbon-14 and the uranium isotopes in Mobility Class 2 were considered to be in sufficient quantity and mobile enough to warrant a detailed analysis of groundwater impacts. Although three of the constituents in Mobility Class 1— selenium, chloride, and tritium—are considered very mobile, they were screened out for other factors. Selenium and chloride were not considered in the assessment because the total inventories for both of these constituents were estimated to be less than  $1 \times 10^{-2}$  Ci. Tritium was not evaluated because of its relatively short half-life.

Estimated inventories of hazardous chemical constituents associated with LLW and MLLW disposed of after 1988 being considered under each alternative group would be expected to be found at trace levels. MLLW, which would be expected to contain the majority of hazardous chemical constituents, would undergo predisposal solidification to stabilized waste forms and containment and thermal treatment to remove organic chemical components of the MLLW. This waste treatment would be done to meet current waste acceptance criteria and land disposal restrictions before being disposed of in permitted MLLW facilities. Consequently, groundwater quality impacts from these constituents would not be expected to be substantial.

Analysis of MLLW inventories for this assessment did identify two exceptions that included lead and mercury inventories associated with the projected MLLW that were estimated at 336 kg (741 lb) and 2.5 kg (5.5 lb), respectively. Because of its affinity to be sorbed into Hanford sediments, lead falls within Mobility Class 5 ( $K_d = 40$  mL/g) and would not release to groundwater within the 10,000-year period of interest. The inventory estimated for mercury is assumed to be small enough that it would not release to groundwater in substantial concentrations. Even the most conservative estimates of release would yield estimated groundwater concentrations at levels two orders of magnitude below the current standard of 0.002 mg/L.

1 LLW disposed of prior to September 1987 may contain hazardous chemical constituents, but no  
2 specific requirements existed to account for or report the content of hazardous chemical constituents in  
3 this category of LLW. As a consequence, analysis of these constituents and estimated impacts based on  
4 the limited amount of information on estimated inventories and waste disposal locations would be subject  
5 to uncertainty at this time. These facilities are part of the LLW and MLLW facilities in the LLW  
6 Management Areas 1 – 4 that are currently being monitored under RCRA interim status programs. Final  
7 evaluation of these facilities under RCRA and/or CERCLA guidelines would eventually require analysis  
8 of the impacts of the chemical components of these inventories. Any analysis with information that is  
9 currently available would be at best speculative without more detailed inventory characterization informa-  
10 tion. Such analyses would require a more thorough and detailed characterization of these wastes at some  
11 future date.

### 12 13 **G.1.3.2 Source Inventories**

14  
15 The sources inventories of key constituents that provided the basis for water quality impacts  
16 described in this appendix and Section 5.3 are summarized by alternative group in Appendix B. The  
17 inventory associated with the specific constituents for each of alternatives was partitioned between the  
18 200 East and West Areas roughly in proportion to estimated disposal areas in the LLBGs that had already  
19 received LLW or will receive newly generated LLW. Estimates of LLBG areas for all the alternatives are  
20 summarized in Section 5.1, Table 5.1. Distribution of LLBGs for each waste category assumed in the  
21 release modeling, described in the section below, in the HSW disposal site areas by alternative are given  
22 in Table G.2. The broad categories considered include previously disposed LLW, newly generated Cat 1  
23 and Cat 3 LLW, and MLLW. The relative percentages of LLBG areas for these three categories provide  
24 the basis for the partitioning of LLW volumes and associated constituent inventories. For purposes of this  
25 analysis, the greater-than-Cat 3 (GTC3) LLW were considered part of the Cat 3 LLW inventory.  
26 Although no specific GTC3 LLW is expected in forecasted wastes, for purposes of this analysis, it was  
27 assumed that about 1 m<sup>3</sup> (1.4 yd<sup>3</sup>) of GTC3 LLW containing mostly cesium-137 and other non-mobile  
28 nuclides would be part of the inventory considered. The inventory of this category is included in the  
29 Cat 3 LLW and is not discussed separately.

### 30 31 **G.1.3.3 Release Models**

32  
33 Source-release models were selected and used to approximate contaminant releases from the variety  
34 of LLW types considered in this analysis. The models considered included a soil-debris release model  
35 and a cement release model.

#### 36 37 **G.1.3.3.1 Soil-Debris Model**

38  
39 In the soil-debris model, LLW is assumed to be mixed with soils. Waste sources included in this  
40 model were assumed to be permeable to percolating water. Thus, all surfaces of the waste were assumed  
41 to come into contact with percolating water. If contaminant inventories in the source were high enough,  
42 leaching of the contaminant through the bottom of the source was controlled by the solubility of the  
43 contaminant in soil water. Otherwise, leaching was controlled by partitioning of the radionuclides  
44 between aqueous and sorbed phases. The inventory was assumed to be perfectly mixed throughout the

**Table G.2.** Assumed Distribution of LLBG Areas (ha) of Previously Disposed of LLW, Cat 1 LLW, Cat 3 LLW, MLLW, and Melters in the 200 East and 200 West Areas by Alternative Group

Disposal Alternative	Previously Disposed of LLW						Category 1 LLW				Category 3 LLW				MLLW				Melters
	1962-1970 LLW		1970-1988 LLW		1988-1995		1996 to 2007		After 2007		1996 to 2007		After 2007		1996 to date and future	After 2007			
	200 East	200 West	200 East	200 West	200 East	200 West	200 East	200 West	200 East	200 West	200 East	200 West	200 East	200 West or ERDF		200 East	200 West or ERDF	200 East	
A (Lower bound Volume)	7.1	2.2	20.9	16.6	19.6	39.7		39.7		4.4		39.7		4.4		1.7		1.5	6.0
A (Hanford Only Volume)	7.1	2.2	20.9	16.6	19.6	39.7		39.7		4.4		39.7		4.4		1.7		1.5	6.0
A (Upper Bound Volume)	7.1	2.2	20.9	16.6	19.6	39.7		39.7		8.9		39.7		8.9	3.5	1.7		3.0	6.0
B (Lower bound Volume)	7.1	2.2	20.9	16.6	19.6	39.7		39.7	0.7	16.7		39.7	0.7	16.7		1.7	5.7		6.0
B (Hanford Only Volume)	7.1	2.2	20.9	16.6	19.6	39.7		39.7	0.7	16.7		39.7	0.7	16.7		1.7	5.7		6.0
B (Upper Bound Volume)	7.1	2.2	20.9	16.6	19.6	39.7		39.7	4.0	25.1		39.7	1.1	28.0	3.5	1.7	10.2		6.0
C (Lower bound and Hanford Volume)	7.1	2.2	20.9	16.6	19.6	39.7		39.7		4.4		39.7	0.0	4.4		1.7	1.5		6.0
C (Hanford Only Volume)	7.1	2.2	20.9	16.6	19.6	39.7		39.7		4.4		39.7	0.0	4.4		1.7	1.5		6.0
C (Upper Bound Volume)	7.1	2.2	20.9	16.6	19.6	39.7		39.7		8.9		39.7	0.0	8.9	3.5	1.7	3.0		6.0
D1, D2, and D3 (Lower bound Volume)	7.1	2.2	20.9	16.6	19.6	39.7		39.7	3.0			39.7	3.0			1.7	1.1		6.0
D1, D2, and D3 (Hanford Only Volume)	7.1	2.2	20.9	16.6	19.6	39.7		39.7	3.0			39.7	3.0			1.7	1.1		6.0
D1, D2, and D3 (Upper Bound Volume)	7.1	2.2	20.9	16.6	19.6	39.7		39.7	6.2			39.7	6.2		3.5	1.7	3.0		6.0
E1, E2, and E3 (Lower Bound Volume)	7.1	2.2	20.9	16.6	19.6	39.7		39.7	3.0			39.7	3.0			1.7	1.1		6.0
E1, E2, and E3 (Hanford Only Volume)	7.1	2.2	20.9	16.6	19.6	39.7		39.7	3.0			39.7	3.0			1.7	1.1		6.0
E1, E2, and E3 (Upper Bound Volume)	7.1	2.2	20.9	16.6	19.6	39.7		39.7	6.2			39.7	6.2		3.5	1.7	3.0		6.0
No Action	7.1	2.2	20.9	16.6	19.6	39.7		39.7		39.7		39.7			3.5	1.7	3.0		6.0

1 source volume during the entire release period—assuming perfectly mixed conditions reduced the  
2 likelihood that solubility would control the release. The mathematical basis of this release model is  
3 described in detailed in Appendix D of Kincaid et al. (1998).

4  
5 The soil-debris model was used to estimate release of all non-grouted contaminants from previously  
6 disposed of LLW, Cat 1 LLW, Cat 3 LLW, and MLLW. The key parameter in the use of the soil-debris  
7 release model, besides the depth of the waste, is the rate of infiltrating water through the LLBGs.  
8 Table G.3 provides a summary of assumed waste depths and infiltration rates used in the soil-debris  
9 model for each alternative.

10  
11 This assessment focuses on the long-term release of contaminants from new LLBGs during the post-  
12 closure period. This assumption of minimal leaching and migration prior to site closure is reasonable for  
13 the majority of LLW and MLLW being considered. Containment and waste forms used in Cat 1 and  
14 Cat 3 LLW would be expected to be sufficient to contain and isolate disposed LLW during the  
15 operational period. MLLW facilities, which involve the collection and management of leachate during  
16 and following the operational period, are also expected to control the amount of waste leaching during the  
17 period of operations. Thus, an infiltration rate of 0.5 cm/yr was used for the Cat 1 LLW, Cat 3 LLW, and  
18 MLLW within the No Action Alternative.

19  
20 Because less rigorous requirements for waste contaminant and content were in effect prior to 1988,  
21 contaminants contained in solid LLW disposed of in LLBGs prior to 1988 offer the highest potential for  
22 leaching and release into the vadose zone prior to site closure. This analysis evaluated the potential  
23 impacts of these earlier disposals by evaluating the effect of higher infiltration rates during the period of  
24 operations. The leaching of these categories of LLW prior to site closure has the potential to be influ-  
25 enced by relatively high infiltration rates during and shortly after the disposal period when bare soil  
26 conditions persist. Infiltration rates into coarse surface sediments maintained free of vegetation, as would  
27 be expected during and shortly after the disposal period, is estimated to be in the order of 5 cm/yr, based  
28 on data from a non-vegetated gravel-covered lysimeter study conducted on the Hanford Site (Fayer and  
29 Walters 1996; Fayer et al. 1999). Eventually, infiltration through the LLBGs would be expected to be  
30 reduced to lower levels as surface cover conditions return to a more natural vegetative state.

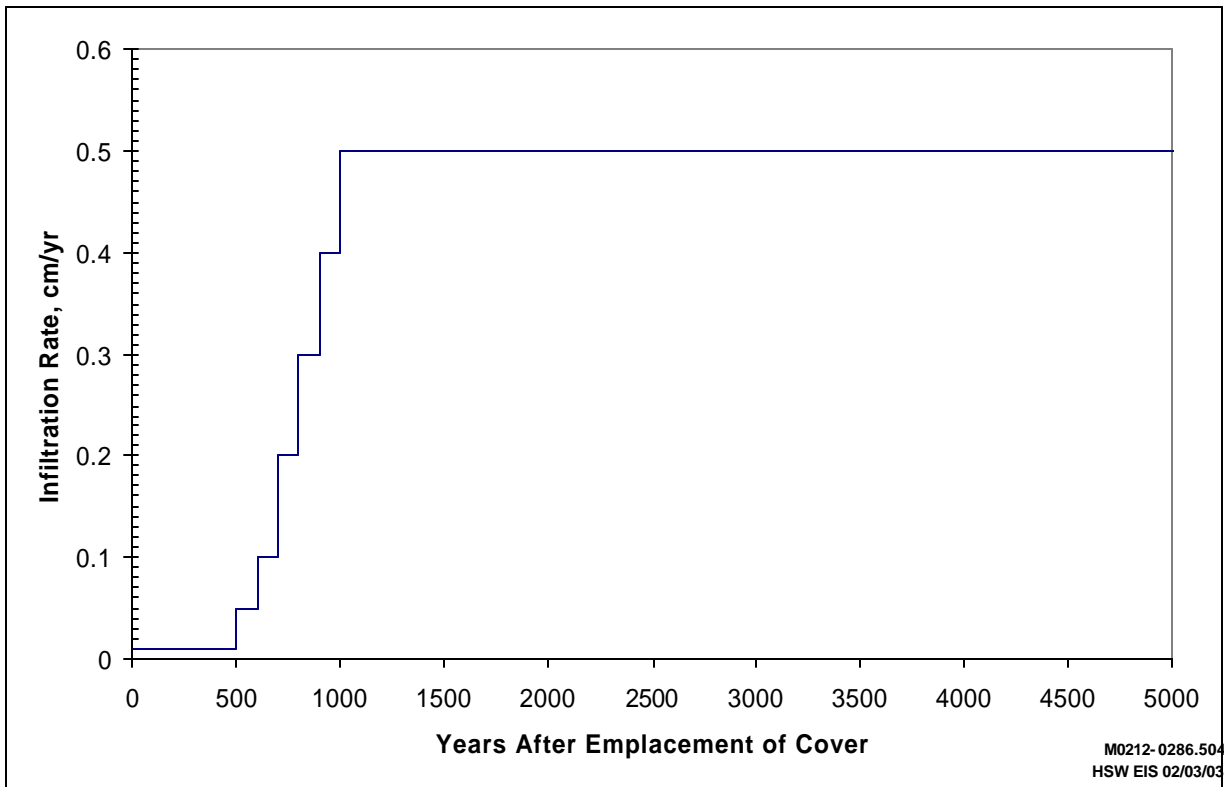
31  
32 For the No Action Alternative, an infiltration rate used in release modeling of the pre-1970 and 1970-  
33 1988 LLW was increased to 0.5 cm/yr after the operational period and during the post-closure period.  
34 This infiltration rate is a reasonable rate (Fayer and Walters 1996; Fayer et al. 1999) to use in the post-  
35 closure period when natural vegetative cover would be expected to persist.

36  
37 For all LLW and MLLW under all action alternatives, it is assumed that LLBGs would have a long-  
38 term surface barrier at site closure that would limit infiltration rates through the disposed wastes. The  
39 assumed barrier is a modified RCRA Subtitle C cover system. Recharge from this barrier system is  
40 expected to be very low and comparable to long-term recharge estimates for the Hanford Protective  
41 Barrier. A recent analysis by Fayer et al. (1999) for the ILAW Disposal Program has estimated a long-  
42 term infiltration at 0.01 cm/yr through this type of a system with an established natural (that is, shrub-  
43 steppe plant community) cover condition.

**Table G.3.** Summary of Waste Depth and Infiltration Rates Used in the Soil-Debris Release Model

	Waste Depth (meters)	Infiltration Used in Waste Release Models (cm/yr)							
		Prior to 2046	2046-2546	2547-2646	2647-2746	2747-2846	2847-2976	2947-2946	3046 -12046
<b>Action Alternatives</b>									
<b>Wastes Disposed of prior to 1995</b>									
Pre-1970	6	5	0.01	0.05	0.1	0.2	0.3	0.4	0.5
1970-1987	6	5	0.01	0.05	0.1	0.2	0.3	0.4	0.5
1988-1995	6	5	0.01	0.05	0.1	0.2	0.3	0.4	0.5
<b>Wastes Disposed of between 1996 and 2007</b>	6	n/a	0.01	0.05	0.1	0.2	0.3	0.4	0.5
<b>Wastes Disposed of after 2007</b>									
Alt Group A	15.6	n/a	0.01	0.05	0.1	0.2	0.3	0.4	0.5
Alt Group B	6	n/a	0.01	0.05	0.1	0.2	0.3	0.4	0.5
Alt Group C	15.6	n/a	0.01	0.05	0.1	0.2	0.3	0.4	0.5
Alt Group D <sub>1</sub>	15.6	n/a	0.01	0.05	0.1	0.2	0.3	0.4	0.5
Alt Group D <sub>2</sub>	15.6	n/a	0.01	0.05	0.1	0.2	0.3	0.4	0.5
Alt Group D <sub>3</sub>	15.6	n/a	0.01	0.05	0.1	0.2	0.3	0.4	0.5
Alt Group E <sub>1</sub>	15.6	n/a	0.01	0.05	0.1	0.2	0.3	0.4	0.5
Alt Group E <sub>2</sub>	15.6	n/a	0.01	0.05	0.1	0.2	0.3	0.4	0.5
Alt Group E <sub>3</sub>	15.6	n/a	0.01	0.05	0.1	0.2	0.3	0.4	0.5
<b>Melter Trench(All Alternatives Groups)</b>	18.6	n/a	0.01	0.05	0.1	0.2	0.3	0.4	0.5
<b>No Action Alternative</b>									
<b>Wastes Disposed of prior to 1995</b>									
Pre-1970	6	5	0.5	0.5	0.5	0.5	0.5	0.5	0.5
1970-1987	6	5	0.5	0.5	0.5	0.5	0.5	0.5	0.5
1988-1995	6	5	0.5	0.5	0.5	0.5	0.5	0.5	0.5
<b>Wastes Disposed of after 1996</b>	6	n/a	0.5	0.5	0.5	0.5	0.5	0.5	0.5
N/A = Not applicable.									

1 No guidance is available for specifying barrier performance after its design life. However, an  
2 immediate decrease in performance is not expected, and it is likely that this specific barrier will perform  
3 as designed far beyond its design life. Without data to understand and predict long-term performance of  
4 the specific barrier, a conservative assumption is the performance of the barrier would degrade stepwise  
5 after reaching its design life, and until the recharge rate matches the natural recharge rate in the surround-  
6 ing environment. This approach is based on the assumption that a degraded cover will eventually return  
7 back to its natural state and behave like the surrounding environment. The period of degradation was  
8 assumed to be the same as the design life. At the time of site closure, all waste disposal facilities are  
9 assumed to be covered with the modified RCRA Subtitle C cover system. To approximate the effect of  
10 the cover on waste release, the following assumed infiltration rates, as illustrated in Figure G.3, were used  
11 in the waste release modeling. For 500 years after site closure, an infiltration rate of 0.01 cm/yr was used  
12 to approximate the effect of cover emplacement over the wastes and its impact on reducing infiltration.  
13 After 500 years, the cover is assumed to begin to degrade. Between 500 to 1000 years after site closure,  
14 infiltration rates were increased linearly from 0.01 cm/yr to 0.5 cm/yr to approximate a 500-year period of  
15 cover degradation and a return infiltration rate reflective of natural vegetated surface soil conditions over  
16 the wastes. The final rate of 0.5 cm/yr was used for the remaining 9000-year period of analysis.  
17



18  
19  
20 **Figure G.3.** Changes in Infiltration Rates Assumed in Source-Term Release to Approximate the  
21 Modified RCRA Subtitle C Cover System Degradation

1 A number of the alternatives considered specify the use of liner systems to control waste release  
2 during the period of operations. However, no credit for the effect of these liner systems was considered in  
3 this long-term analysis. Although the liner systems as described in Section 3.1 might last (that is, contain  
4 leachate for removal) for several hundreds of years if properly managed, this analysis assumed that the  
5 emplaced liners would fail during the 100-year active institutional control period and would have little  
6 effect on the long-term waste release during the 10,000-year period of analysis  
7

8 In the case of uranium isotope release calculations, sufficient inventories of uranium in a number of  
9 LLW categories were estimated with the soil-debris model using solubility controls. For all LLW  
10 categories except Cat 3 LLW, a solubility-controlled concentration of 64 mg/L was used for all uranium  
11 isotopes. This estimate was developed and described for Hanford-specific conditions in Wood et al.  
12 (1996) for use in the performance assessment of solid waste burial grounds in the 200 East Area.  
13

14 In the Cat 3 LLW, the geochemical environment created by the presence of cement associated with  
15 the high-integrity containers (HIC) and the in-trench grouting is expected to reduce the release of uranium  
16 at much lower concentration limits. The solubility-controlled concentration used for Cat 3 LLW was  
17 0.23 mg/L, which was based on an estimate ( $2.34 \times 10^{-4}$  g/L) developed and described in Wood et al.  
18 (1996) for use in the performance assessment of solid waste burial grounds in the 200 East Area.  
19

20 To account for the expected delay in release of Cat 3 LLW, because it is contained within HICs or  
21 grouted in place, the soil-debris release model used a 300-year delay before releases were initiated. This  
22 delay is consistent with the estimated 300-year lifetime of LLW containment effectiveness of the HIC or  
23 in-trench grouting.  
24

25 For some categories (Cat 3 LLW and Cat 3 MLLW) in each of the alternatives, LLW containing  
26 elevated levels of technetium-99 will be placed in a grout matrix before being placed in the LLBGs. For  
27 this type of grouted waste, a release model referred to as the cement-release model was used to  
28 approximate the source release. The underlying basis of the cement-release model assumes that (1) the  
29 permeability of the grouted waste is much lower than that of the surrounding soil, (2) the permeability of  
30 the waste is low enough that advective water flow within the waste form is essentially zero, and (3) the  
31 pore space connectivity in the cementitious waste form is sufficiently high enough to allow contaminant  
32 mobility within the waste form by diffusion. The mathematical basis of this release model is also  
33 described in detailed in Appendix D of Kincaid et al. (1998).  
34

35 In the cement-release model, percolating water is assumed to move around the grouted waste, and  
36 contaminants are leached only from the outer surface. As this occurs, contaminants inside the waste form  
37 are assumed to diffuse toward the outer surface. Therefore, overall contaminant release from the source  
38 zone is assumed to be controlled by the effective diffusion coefficient of the contaminant in the waste  
39 form.  
40

## Effect of Organic Hazardous Chemicals on Long-term Water Quality Impacts

The effect of hazardous chemicals, particularly organic chemicals, on enhancing the mobility of normally sorbed or immobile constituents in transport was raised as an important technical issue for solid waste disposal facilities during public review and comment of the first draft HSW EIS. Detailed evaluations of tabulations of metal-organic complex stability constants for organic compounds (Martell 1971; Martell and Smith 1977; Smith and Martell 1982) suggest that most of the stability constants are weak for organics typically contained in LLW and MLLW. The more typical organic compounds found in LLW and MLLW are non-polar and relatively hydrophobic molecules. Organics that fit into this category (that is, carbon tetrachloride, trichloroethane, and other volatile organics) generally cannot form a complex with metals and radionuclides and enhance their mobility. However, such non-polar and/or hydrophobic organic compounds if disposed in large quantities and in high concentration could potentially affect radionuclide and metal migration by creating a reducing zone in the sediments or groundwater especially if biological activity is occurring. Field evidence suggests that this has not occurred to any significant extent at any waste site at Hanford (see Serne and Wood 1990 and references therein). Thus this type of enhanced transport is not expected to be important in affecting field-scale transport of constituents of concern from HSW EIS disposal sites. A small subset of organic compounds, commonly referred to as complexing/chelating agents, do have the ability to enhance the mobility of some normally sorbed or immobile constituents. Some notable examples of such agents include ETDA, HEDTA, DTPA, oxalic acid, and TBP. The ability of these complexing agents to affect the general mobility of normally immobile or sorbed radionuclides and metals is a function of many factors, including:

- The type and amount of organic complexing agent is present
- The stability of the complex and the kinetics of its formation and disassociation back to free molecules
- pH, REDOX and microbiological conditions
- The amount of free liquids or fluids contained within the wastes.

In one instance onsite, the presence of complexing agents (EDTA and/or ferro-ferric-cyanide) in a liquid waste stream discharged to the ground is suspected of enhancing the transport of a cobalt-60 plume from the northern part of the 200 East Area. However, the combination of complexing agents and liquid discharge at this waste site is unique and cannot be interpreted as being representative of expected geochemical or vadose zone flow and transport conditions that would be expected at solid waste burial grounds.

At this time, there is no specific evidence that would support enhanced movement of moderately to strongly sorbed radionuclides or metals (for example, cesium, strontium, europium, uranium, or plutonium) due to the presence of organic complexing agents in solid wastes within LLBGs. In fact, no field-scale evidence has been found at other solid waste LLW sites across North America that would support this hypothesis (Serne et al. 1990 and 1995). Estimated inventories of hazardous chemical constituents and particular organic complexing agents associated with LLW and MLLW disposed of after 1988 are thought to be quite small. MLLW, which would be expected to contain the majority of hazardous chemical constituents, will undergo predisposal solidification to stabilize waste forms and thermal treatment to remove organic chemical components of the MLLW. This waste treatment would be done to meet current waste acceptance criteria and land disposal restrictions before disposal in permitted MLLW facilities. Consequently, the effect of organic complexing agents and groundwater quality impacts from organic chemicals, in general, would not be expected to be substantial for solid wastes.

LLW disposed of prior to September 1987 may potentially contain hazardous chemical constituents and organic complexing agents, but because no specific requirements existed to account for or to report their content, it is difficult to assess impacts. As a consequence, analysis of these constituents and estimated impacts based on the limited amount of information on estimated inventories and waste disposal location would be subject to large uncertainty at this time. These facilities are part of the LLW and MLLW facilities in the LLW Management Areas 1 – 4 that are currently being monitored under RCRA interim status programs. Final evaluation of these facilities under RCRA and/or CERCLA guidelines would eventually require analysis of the impacts of the chemical components of these disposed inventories. Any analysis with information that is currently available would be at best speculative without more detailed inventory characterization information. Such analyses would require a more thorough and detailed characterization of these wastes at some future date or more extensive vadose zone monitoring (that is, extraction of pore fluids underneath the burial grounds). There is no evidence of enhanced mobility of radionuclides or chemicals, which can be traced back to the solid wastes, in groundwater surrounding the monitoring wells that surrounding the LLBGs.

**Relation of the HSW-EIS to Current Performance Assessments  
for LLW and MLLW Disposal**

The long-term radiological impacts of solid wastes disposed of in LLBGs in the 200 East and West Areas since October 1987 have been evaluated with two active performance assessments (*Performance Assessment for the Disposal of Low-Level Waste in the 200 West Area Burial Grounds* [Wood et al. 1995] and *Performance Assessment for the Disposal of Low-Level Waste in the 200 East Area Burial Grounds* [Wood et al. 1996]). These performance assessments were approved by DOE (Cowan 1996; Frei 1997).

The proposed disposal of immobilized low-activity waste (ILAW) derived from the Tank Waste Treatment Plant in a disposal facility sited southwest of the PUREX Plant within the 200 East Area has also been evaluated using a performance assessment (Mann et al. 2001). This performance assessment was also approved (DOE 2001). Ongoing maintenance for all three of these performance assessments includes continual evaluation and production of annual reports on new data and information on projected disposal inventories, geochemical, and waste form performance data and information and their relevance to current performance assessment results and conclusions

Projected waste inventories, selection of disposal methods, or trench designs that might result from this HSW EIS would be addressed under performance assessment compliance requirements as specified in DOE Order 435.1. Long-term performance assessment of radiological impacts from disposal facilities is a part of several requirements specified under DOE Order 435.1 for Hanford Site low-level waste disposal facilities to ensure the protection of workers, the public, and the environment.

Analysis of the most current baseline disposal practices that use conventional trenches for both solid wastes and ILAW show that for current waste inventory projections, operational waste acceptance criteria and waste acceptance practices continue to be compliant with performance objectives.

Specific values of the effective diffusion coefficient in cement-release model type waste forms for each radionuclide were chosen from the values originally reported by Serne et al. (1989). These values had previously been incorporated into a computer database known as the Multimedia-Modeling Environmental Database Editor (MMEDE) (Warren and Strenge 1994). For the source-term calculation effort of this analysis, the MMEDE database was queried to produce an electronic file of tabulated diffusion coefficients for relevant radionuclides (that was subsequently incorporated into the source-term calculation spreadsheet). This study used diffusion coefficient values as reported in Buck et al. (1997). Diffusion coefficients of  $1 \times 10^{-11}$  and  $1 \times 10^{-12} \text{ cm}^2 \text{ s}^{-1}$  for technetium-99 and iodine-129, respectively, were used. For some radionuclides (for which no specific values were available), the diffusion coefficient was fixed at a reasonable conservatively high default value ( $5 \times 10^{-8} \text{ cm}^2 \text{ s}^{-1}$ ).

#### **G.1.4 Vadose Zone Modeling**

Contaminants released from the various LLBGs were transported downward through the vadose zone to the water table. The primary mechanism for transport in the vadose zone was water flow in response to gravitational and capillary forces. After the LLW disposal operations cease, steady-state hydraulic conditions resulting from different surface covers (including re-vegetation) that affect recharge were represented in the model. Recharge directly from precipitation or snowmelt infiltrates into the vadose zone. The recharge rate varies for the assumed surface cover conditions for each of the LLBGs. The data used in the vadose zone model are described in the remainder of this section.

The vadose zone was modeled as a stratified one-dimensional column. In this analysis, it was not appropriate to represent the vadose zone as multidimensional because of the large number of LLBG sites

1 modeled and the limited characterization of the vadose zone. Multidimensional modeling of the vadose  
2 zone has been performed for some waste sources and types (Mann et al. 1997; Mann et al. 2001) but was  
3 not practical for this analysis for the large number of sites in question. A one-dimensional approach  
4 would also be expected to yield results that would be more conservative than those produced with multi-  
5 dimensional approaches which consider lateral spreading of infiltration and contaminant transport.

6  
7 The remainder of this section describes the stratigraphy, hydraulic properties, recharge, and  
8 geochemical conditions used in this analysis.

#### 9 10 **G.1.4.1 Stratigraphy**

11  
12 Because of the large number of sites to be modeled in this assessment, the technical approach used for  
13 the vadose zone stratigraphy was similar to the approach used in the Composite Analysis by Kincaid et al.  
14 (1998). The stratigraphy used was an approximation that was consistent with the major geologic forma-  
15 tions found in the vadose zone beneath the Central Plateau in the areas of question and was based on work  
16 documented in Thorne and Chamness (1992), Thorne et al. (1993), and Thorne et al. (1994). In the  
17 composite analysis, the stratigraphies for several areas of the 200 East and 200 West Areas were defined  
18 as a set of strata consistent with the nearest available well log from 18 well logs (Kincaid et al. 1998).  
19 Each of the well logs included location, ground surface elevation, and the thickness of the various major  
20 sediment types.

21  
22 A summary of the geologic well logs used in the composite analysis appears in Table G.4. At each  
23 profile location, seven sediment types, and one rock type (basalt) were identified and used to define the  
24 stratigraphy. The acronyms of the sediment types provided in Table G.5 are associated with the following  
25 sediment types: 200 West Area Hanford Sand (WHS) sediment, 200 West Area Early Palouse (WEP)  
26 sediment, 200 West Area Plio Pleistocene (WPP) sediment, 200 West Area Ringold (WR) sediment,  
27 200 East Area Hanford Sand (EHS) sediment, 200 East Area Ringold (ER) sediment, and 200 East Area  
28 Hanford Gravel (LEHG or EHG) sediment. East Hanford Gravel sediment type also appears in the table  
29 as LEHG, but the same soil moisture characteristics are applied to both. At most, four different sediment  
30 types occurred above the basalt at any location. In the vadose zone model, the basalt rock type was  
31 regarded as impermeable and was used to define the default bottom of the vadose zone profile. If the  
32 water table fell below the top of the basalt, as in the case for LLBGs located in the northern part of the  
33 200 East Area, the vadose zone was still assumed to be limited to the basalt surface.

34  
35 Two of the composite well logs developed for the composite analysis were selected for use in this  
36 assessment based on their proximity to the LLBGs. The specific well logs used to approximate the  
37 vadose zone stratigraphy at the LLBGs, which are noted in the first two rows of the table, are 218-E-12b  
38 in the 200 East Area and 218-W-5 in the 200 West Area and the ERDF.

#### 39 40 **G.1.4.2 Hydraulic Properties**

41  
42 Modeling water flow and radionuclide transport through the vadose zone required a description of the  
43 relationship among moisture content, pressure head, and unsaturated hydraulic conductivity. These  
44 relationships, called soil moisture characteristics, are highly nonlinear. In this analysis, non-hysteretic

**Table G.4.** Geologic Well Logs for the Vadose Zone Model

Composite Well Log	Surface Elevation (m)	Northing (m) <sup>(a)</sup>	Easting (m) <sup>(b)</sup>	Sediment 1 <sup>(c)</sup>	Thickness (m)	Sediment 2	Thickness (m)	Sediment 3	Thickness (m)	Sediment 4 <sup>(d)</sup>	Thickness (m)
218-W-5 <sup>(e)</sup>	224.9	137024	565658	WHS	19	WEP	4	WPP	7	WR	85
218-E-12B <sup>(f)</sup>	191.9	137238	574643	EHG	10	EHS	6	LEHG	54	ER	0.01
218-E-10	190.7	137468	572924	EHG	10	EHS	6	LEHG	59	ER	0.01
299-E13-20	226.4	134313	573610	EHG	10	EHS	6	LEHG	80	ER	60
299-E19-1	224.1	135086	572820	EHG	10	EHS	6	LEHG	91	ER	51
299-E24-7	218.2	135561	574407	EHG	10	EHS	6	LEHG	60	ER	56
299-E25-2	205.9	136062	575514	EHG	10	EHS	6	LEHG	60	ER	36
299-E26-8	188.8	136687	575522	EHG	10	EHS	6	LEHG	44	ER	14
299-E28-16	214.3	136562	573135	EHG	10	EHS	6	LEHG	71	ER	12
299-E28-22	213.5	136321	574041	EHG	10	EHS	6	LEHG	83	ER	17
299-W6-1	214.1	137510	567214	WHS	14	WPP	4	WR	121		
299-W11-2	217.8	136671	567407	WHS	34	WEP	4	WPP	7	WR	110
299-W14-7	206.6	135655	567034	WHS	38	WPP	2	WR	118		
299-W14-8A	221.0	135688	568013	WHS	47	WEP	5	WPP	5	WR	106
299-W15-15	212.8	135752	566089	WHS	42	WEP	3	WPP	8	WR	100
299-W18-21	203.8	134979	566098	WHS	36	WEP	5	WPP	3	WR	100
299-W21-1	213.1	134397	568141	WHS	53	WEP	8	WPP	8	WR	100
299-W22-24	211.0	134411	567648	WHS	42	WEP	13	WPP	12	WR	104

(a) Refers to north coordinate in Washington State Plane NAD83 coordinate system.  
 (b) Refers to east coordinate in Washington State Plane NAD83 coordinate system.  
 (c) Refers to the upper sediment layer.  
 (d) Refers to the lowest sediment layer simulated.  
 (e) Composite well log used in analysis of the 200 West Area LLBGs.  
 (f) Composite well log used in analysis of the 200 East Area LLBGs.  
 EHS – 200 East Area Hanford Gravel Sediment.  
 LEHG – Lower 200 East Area Hanford Gravel Sediment.  
 ER – 200 East Area Ringold Sediment.  
 WHS – 200 West Area Hanford Sand Sediment.  
 WPP – 200 West Area Plio-Pleistocene Sediment.  
 WEP – 200 West Area Lower Palouse Sediment.  
 WR – 200 West Area Ringold Sediment.

1 relationships were assumed for Hanford Site soils because few measurements to characterize hysteresis  
2 have been made for such soils, and it is believed to be of secondary importance. The hydraulic properties  
3 of Hanford Site soils are highly variable, both between the Hanford and Ringold formations and within  
4 each of the formations (Khaleel and Freeman 1995). For purposes of this analysis, the values of each of  
5 the parameters provided in the table were the values used.

6  
7 In this analysis, different sediment types were used to define the one-dimensional columns beneath  
8 the LLBGs. The hydraulic properties of the sediment types were assumed to be uniform with each  
9 sediment layer. Preferential flow paths in the form of wells and clastic dikes were not considered in this  
10 analysis because use of one-dimensional models cannot represent their local influence in a three-  
11 dimensional environment. The potential influence of preferential flow paths, especially clastic dikes, has  
12 been addressed in the performance assessments for the solid waste burial grounds (Wood et al. 1995,  
13 1996) and, more recently, by Ward et al. (1997) for post-1988 LLW. Wood et al. (1995) and Wood et al.  
14 (1996) concluded that clastic dikes were insufficiently large and insufficiently continuous to provide a  
15 true preferential pathway.

16  
17 The model of soil hydraulic properties based on the van Genuchten (1980) and Mualem (1976)  
18 analytical expressions was used as the basis for the relationships among moisture content, pressure head,  
19 and unsaturated hydraulic conductivity. This model has been applied in previous vadose zone studies at  
20 the Hanford Site. Parameters for the van Genuchten and Mualem models have been determined by fitting  
21 experimental data for Hanford Site sediments to the classic analytic expressions of these models. These  
22 results are described in several Hanford Site documents, but the parameters used in this analysis were  
23 compiled by Khaleel and Freeman (1995).

24  
25 For this analysis, unsaturated flow parameters were established for each of the vadose zone sediment  
26 types previously defined. Sediment types and the associated unsaturated flow modeling parameters used  
27 in this analysis are shown in Table G.5. It should be noted that laboratory-measured moisture retention  
28 and saturated conductivity data in Table G.5 have been corrected for the gravel fraction (> 2 mm) present  
29 in the bulk sample.

### 30 31 **G.1.4.3 Recharge Rates**

32  
33 This assessment focuses on the long-term transport of contaminants from the LLBGs through the  
34 underlying vadose zone to the unconfined aquifer after the end of the operational period in 2046. At the  
35 Hanford Site, data on the current distribution of soil moisture and contaminants in the vadose zone at the  
36 majority of waste sites are inadequate to define long-term conditions for modeling, so simulations were  
37 begun at the initiation of LLBG release to the vadose zone assumed to start in 2046. Initial conditions in  
38 this analysis were based on expected conditions after the operational period and assumed a steady-state  
39 natural recharge condition with no contaminants in the vadose zone. The assumed long-term recharge  
40 that will govern the migration of contaminants through the vadose zone to the underlying water table will  
41 be controlled by the expected regional surface conditions surrounding the LLBGs dominated by natural  
42 vegetation and is conservatively estimated to be in the order of 0.5 cm/year as currently estimated for  
43 vegetative surface conditions (Fayer and Walters 1996; Fayer et al. 1999). The net recharge or infiltration  
44 rate will vary, representing a range of surface cover conditions from undisturbed surfaces with natural

1 **Table G.5.** Sediment Types and Unsaturated Flow Model Parameters Used in the Composite Analysis<sup>(a)</sup>  
 2

Sedi ment Name (Code)	van Genuchten alpha (-)	van Genuchten n (1/cm)	Residual Water Content (cm <sup>3</sup> /cm <sup>3</sup> )	Saturated Water Content (cm <sup>3</sup> /cm <sup>3</sup> )	Saturated Hydraulic Conductivity (cm/s)	Bulk Density (g/cm <sup>3</sup> )	Gravel % <sup>(b)</sup>
200 East Area Hanford Gravel (EHG)	8.11E-03	1.58	0.0146	0.119	1.76E-03	1.97	41.70
Lower 200 East Area Hanford Gravel (LEHG)	8.11E-03	1.58	0.0146	0.119	1.76E-03	1.97	41.70
200 East Area Hanford Sand (EHS)	1.30E-01	2.10	0.0257	0.337	1.19E-02	1.78	17.30
200 East Area Ringold (ER)	8.19E-03	1.53	0.0262	0.124	3.97E-04	2.04	43.30
200 West Area Hanford Sand (WHS)	1.44E-02	2.20	0.0519	0.382	3.98E-04	1.64	3.60
200 West Area Early Palouse (WEP)	6.27E-03	2.53	0.0300	0.379	9.69E-05	1.68	2.00
200 West Area Plio-Pleistocene (WPP)	1.55E-02	1.78	0.0616	0.337	5.79E-02	1.65	8.40
200 West Area Ringold (WR)	3.14E-02	1.65	0.0236	0.226	5.76E-02	2.04	43.30
(a) Data are from Khaleel and Freeman (1995). A normal distribution was assumed for the parameters "van Genuchten n," "Residual Water Contents," and "Saturated Water Content," and the mean was calculated accordingly. A log-normal distribution was assumed for the parameters "van Genuchten alpha" and "Saturated Hydraulic Conductivity," and the mean was calculated accordingly. If the sample size was less than 10, the parameters "van Genuchten alpha" and "Saturated Hydraulic Conductivity" were determined using the geometric mean. (b) Only fine particles were assumed to contribute to sorption of contaminants of concern. The impact of larger particles was corrected using gravel %.							

3  
 4 vegetation, to disturbed surfaces maintained free of vegetation, to engineered surface barriers designed for  
 5 long-term service.

6  
 7 **G.1.4.4 Distribution Coefficients**  
 8

9 In this analysis, the linear sorption isotherm model was used in transport calculations. This model  
 10 was selected because it was the only approach for which model parameters (distribution coefficients)  
 11 were available for the LLBG contaminants. The distribution coefficients ( $k_d$ ) used for the vadose zone  
 12 analysis are summarized in Table G.1.

13  
 14 **G.1.4.5 Vadose Zone Model Implementation**  
 15

16 The vadose zone flow and transport model was implemented with the STOMP code (White and  
 17 Oostrom 1996; White and Oostrom 1997; Nichols et al. 1997). Implementation of the vadose zone model

1 with a unit release resulted in estimates of the annual contaminant flux to the water table that were used in  
2 the convolution integral method for linear superposition described previously.

3  
4 The STOMP code was developed under the Volatile Organic Compounds (VOC) Arid Demonstration  
5 Project through the DOE Office of Technology Development (White and Oostrom 1997). STOMP is  
6 based on the numerical solution of the three-dimensional Richards' equation for fluid flow (Richards  
7 1931) and the advection-dispersion equation for contaminant transport. Although STOMP is capable of  
8 three-dimensional simulations, it is also designed to be efficient in performing one- and two-dimensional  
9 simulations. The code is based on an integral-volume, finite-difference method and is designed to  
10 simulate a wide variety of multidimensional, nonlinear, nonisothermal, and multiphase situations.  
11 STOMP was selected for this analysis because of computational efficiency and flexibility, its prior  
12 application to the Hanford Site vadose zone (Ward et al. 1997), and its thorough documentation (Nichols  
13 et al. 1997), (White and Oostrom 1997), and (White and Oostrom 1996).

14  
15 Because of the large number of sites to be modeled in this assessment, the technical approach used for  
16 the vadose zone stratigraphy was similar to the approach used in the composite analysis by Kincaid et al.  
17 (1998). The stratigraphy used was an approximation that was consistent with the major geologic  
18 formations found in the vadose zone beneath the Central Plateau in the areas of question and was based  
19 on work documented in Thorne and Chamness (1992), Thorne et al. (1993), and Thorne et al. (1994). A  
20 summary of the geologic well logs used in the composite analysis appears in Table G.5. To approximate  
21 the vadose zone at the LLBGs in the 200 East and West Areas, two of the composite well logs developed  
22 for the composite analysis were selected for use in this assessment based on their proximity to the  
23 LLBGs. The specific well logs used to approximate the vadose zone stratigraphy at the LLBGs, which  
24 are noted in the first two rows of the table, are 218-E-12b in the 200 East Area and 218-W-5 in the  
25 200 West Area and the ERDF.

26  
27 Water table elevations for future conditions at the LLBGs were calculated with the groundwater flow  
28 model. This information was used in the vadose zone transport calculations to define the bottom of the  
29 vadose zone. The elevation of the top of the vadose zone at the LLBGs was calculated from land surface  
30 elevations and depth to the bottom of the source, which was tabulated for the LLBG areas.

31  
32 Results of vadose zone transport of a unit release to the water table for the assumed long-term  
33 recharge rate of 0.5 cm/year using assumed soil columns and properties in the 200 East and West Areas is  
34 presented in Figure G.4. Average travel times for the releases of unit mass of contaminants within  
35 Mobility Class 1, as defined by the arrival of 50 percent of each unit mass, is on the order of 500 to  
36 600 years in the 200 East Area and 800 to 900 years in the 200 West Area.

### 37 38 **G.1.5 Groundwater Modeling**

39  
40 Contaminant transport through the saturated unconfined aquifer was simulated with the sitewide  
41 groundwater flow and transport model, CFEST model (Cole et al. 2001a) for the 200 East and the  
42 200 West LLBGs.

LLBG - Low-Level  
Burial Grounds  
STOMP -  
Subsurface  
Transport Over  
Multiple Phases

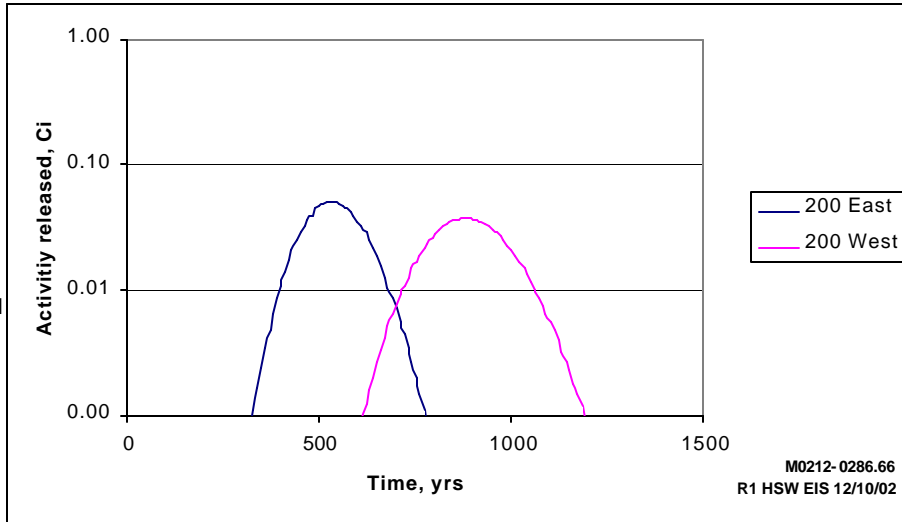


**Figure G.4.** STOMP Code Results for Releases to the Water Table for a Unit Release from LLBGs for an Assumed Recharge Rate of 0.5 cm/yr

A three-dimensional conceptual model was developed for the unconfined aquifer that included stratigraphy, the upper and lower aquifer boundaries, and a table of material units and corresponding flow and transport parameters. The conceptual model was used to guide the setup of the numerical model. A grid spacing of 375 m (1230 ft) was established for the Hanford Site and overlain onto a site map containing physical features and the LLBGs.

### G.1.5.1 Conceptual Model

#### G.1.5.1.1 Hydrogeologic Framework

Hydrogeologic units defined for use in the model were designated by numbers and are briefly described in Table G.6. More detailed descriptions of the sediments were presented in Section 4.5 of this HSW EIS, and a graphic comparison of the model units taken from Thorne et al. (1993) against the stratigraphic column defined in Lindsey (1995) is shown in Figure G.5.

Although nine hydrogeologic units were defined, only seven (Units 1, 4, 5, 6, 7, 8, and 9) are found below the water table during post-Hanford conditions (Cole et al. 1997). Odd-numbered Ringold model units (5, 7, and 9) are predominantly coarse-grained sediments. Even-numbered Ringold model units (4, 6, and 8) are predominantly fine-grained sediments with low permeability. The Hanford formation

**Table G.6.** Major Hydrogeologic Units Used in the Sitewide Three-Dimensional Model

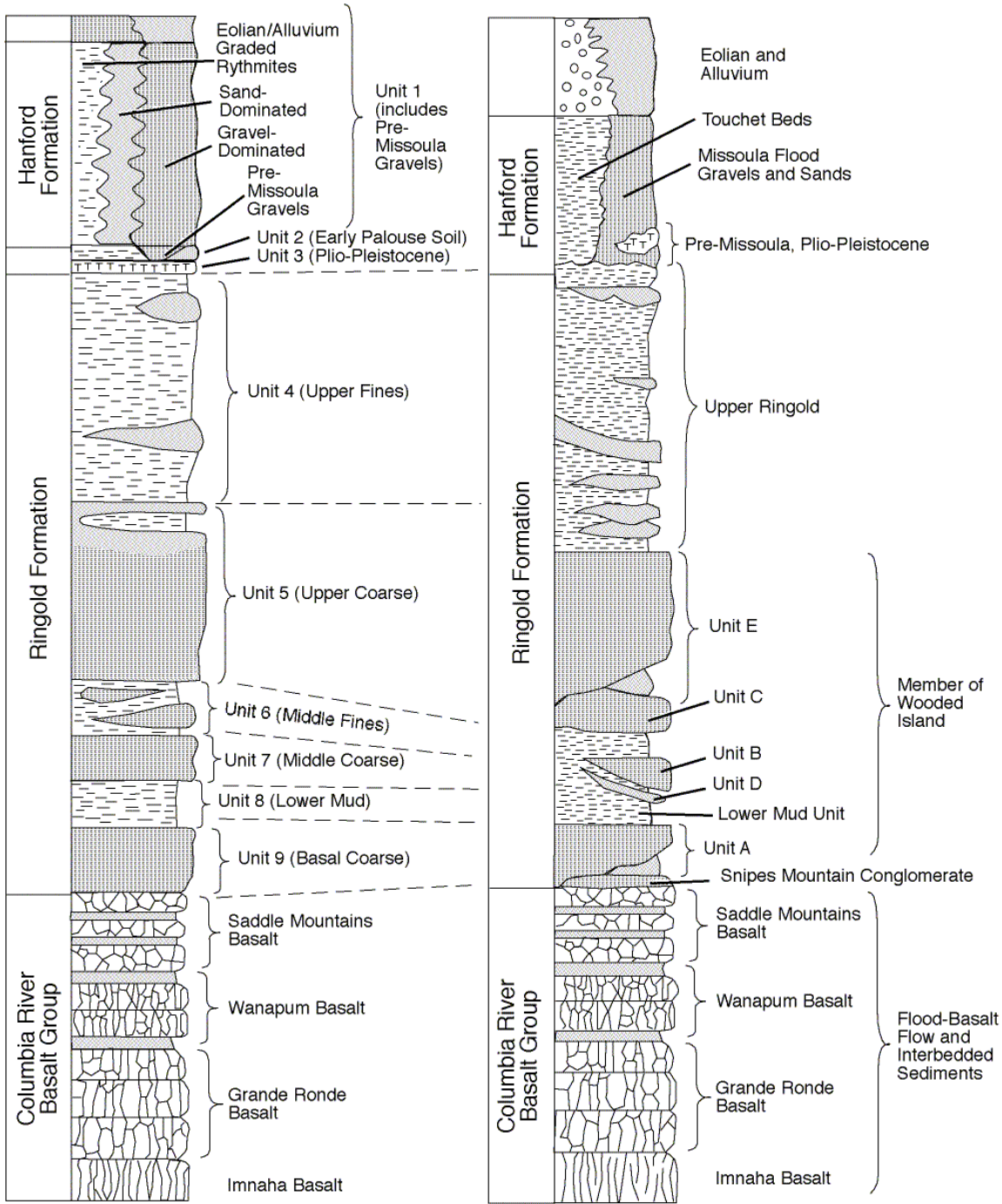
Unit Number	Hydrogeologic Unit	Lithologic Description
1	Hanford Formation	Fluvial gravels and coarse sands
2	Palouse Soils	Fine-grained sediments and eolian silts
3	Plio-Pleistocene Unit	Buried soil horizon containing caliche and basaltic gravels
4	Upper Ringold Formation	Fine-grained fluvial/lacustrine sediments
5	Middle Ringold (Units E and C)	Semi-indurated coarse-grained fluvial sediments
6	Middle Ringold (Lower Ringold Mud)	Fine-grained sediments with some interbedded coarse-grained sediments
7	Middle Ringold (Units B and D)	Coarse-grained sediments
8	Lower Mud Sequence (Lower Ringold and part of Basal Ringold Muds)	Lower blue or green clay or mud sequence
9	Basal Ringold (Unit A)	Fluvial sand and gravel
10	Columbia River Basalt	Basalt

combined with the pre-Missoula gravel deposits were designated as Model Unit 1. Model Units 2 and 3 correspond to the early Palouse soil and Plio-Pleistocene deposits, respectively. These units lie above the current water table. The predominantly mud facies of the upper Ringold unit identified by Lindsey (1995) was designated Model Unit 4. However, a difference in the definition of model units was the lower, predominantly sand, portion of the upper Ringold unit described in Lindsey (1995) was grouped with Model Unit 5 that also includes Ringold gravel/sand Units E and C. This action was taken because the predominantly sand portion of the upper Ringold is expected to have hydraulic properties similar to Units E and C. The lower mud unit identified by Lindsey (1995) was designated Model Units 6 and 8. Where they exist, the gravel and sand Units B and D, found within the lower Ringold, were designated Model Unit 7. Gravels of Ringold Unit A were designated Model Unit 9, and the underlying basalt was designated Model Unit 10. However, the basalt was assigned a very low hydraulic conductivity and was essentially impermeable in the model.

The lateral extent and thickness distribution of each hydrogeologic unit were defined based on information from drillers' well logs, geologists' logs, geophysical logs, and an understanding of the geologic environment. These interpreted areal distributions and thicknesses were then integrated into EarthVision™ (Dynamic Graphics, Inc., Alameda, California), a three-dimensional, visualization software package that was used to construct a database of the three-dimensional hydrogeologic framework.

#### **G.1.5.1.2 Recharge and Flow System Boundary Conditions**

The past development of the sitewide model considered both natural and artificial recharge to the aquifer. Natural recharge to the unconfined aquifer system occurs from infiltration of (1) runoff from elevated regions along the western boundary of the Hanford Site; (2) spring discharges originating from the basalt-confined aquifer system, also along the western boundary; and (3) precipitation falling across



From PNL-8971

Not to Scale

After BHI-00184

M0212-0286.67  
R1 HSW EIS 12/10/02

RG98120214.14

1  
2  
3

**Figure G.5.** Comparison of Generalized Hydrogeologic and Geologic Stratigraphy

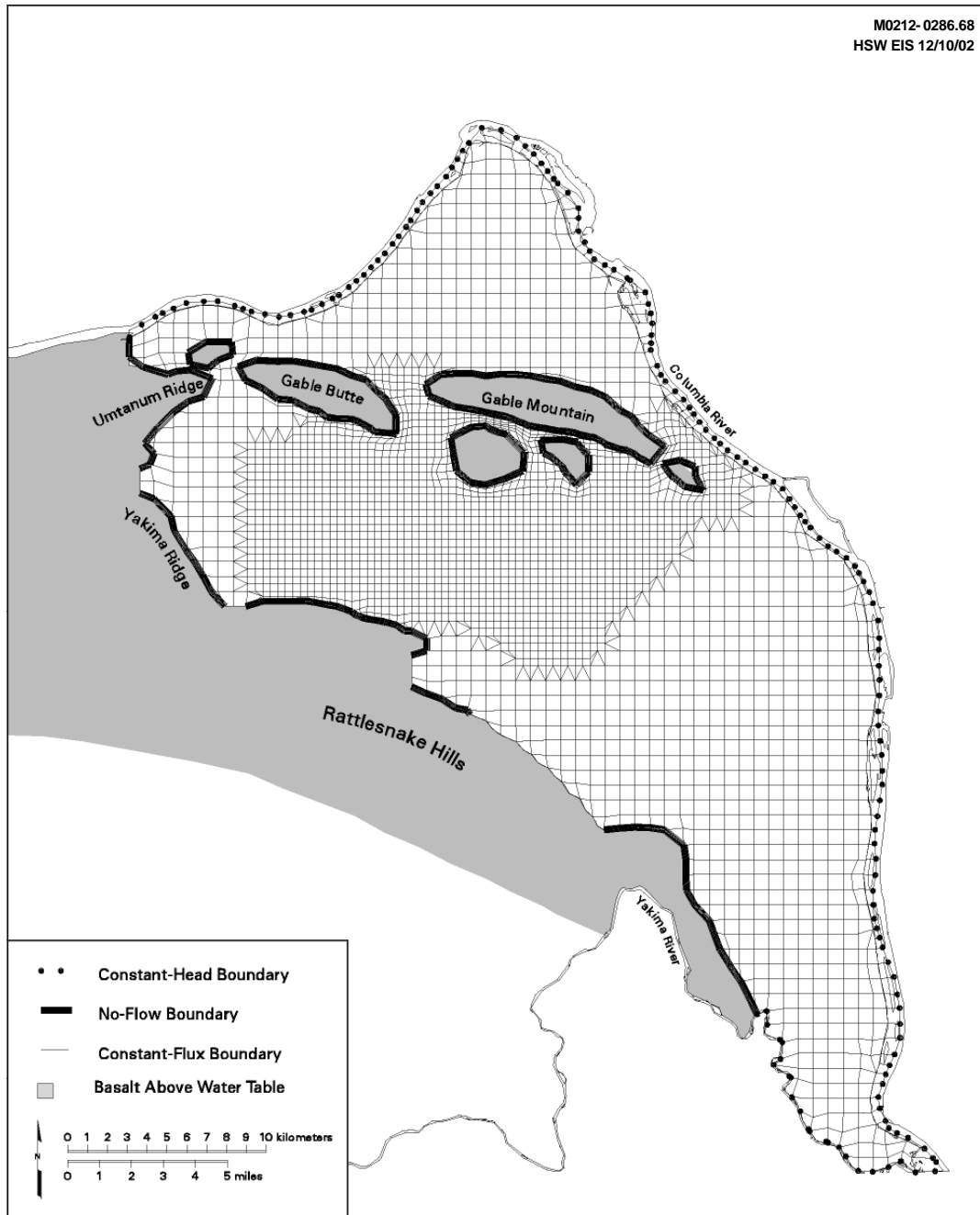
1 the site. Some recharge also occurs along the Yakima River in the southern portion of the site. Natural  
2 recharge from runoff and irrigation in the Cold Creek and Dry Creek Valleys, up-gradient of the site, also  
3 provides a source of groundwater inflow. Natural recharge from precipitation on the site is highly  
4 variable, both spatially and temporally, and depends on local climate, soil type, and vegetation.  
5

6 The other source of recharge to the unconfined aquifer has historically come from wastewater  
7 disposal. The large volume of artificial recharge from wastewater discharged to disposal facilities on the  
8 Hanford Site over the past 60 years has substantially impacted groundwater flow and contaminant  
9 transport in the unconfined aquifer system. This volume of artificial recharge decreased significantly in  
10 the past 10 years, and the water table has been declining steadily over several years. The unconfined  
11 aquifer system eventually will be expected to reach more natural conditions after site closure. Because  
12 flow conditions simulated for this assessment focused on conditions that are likely to exist after Hanford  
13 Site closure and well into the future, the effect of past and current wastewater discharges on the  
14 unconfined aquifer system were not considered in this assessment.  
15

16 Peripheral boundaries defined for the three-dimensional model are shown in Figure G.6, together with  
17 the three-dimensional flow-model grid. The flow system is bounded by the Columbia River on the north  
18 and east and by the Yakima River and basalt ridges on the south and west. The Columbia River  
19 represents a point of regional discharge for the unconfined aquifer system. The amount of groundwater  
20 discharging to the river is a function of local hydraulic gradient between the groundwater elevation  
21 adjacent to the river and the river-stage elevation. This hydraulic gradient is highly variable because the  
22 river stage is affected by releases from upstream dams.  
23

24 Because of the regional-scale nature and long-time frame being considered in the current assessment,  
25 site-wide flow and transport modeling efforts did not attempt to consider the short-term and local-scale  
26 transient effects of the Columbia River system on the unconfined aquifer. However, the long-term effect  
27 of the Columbia River as a regional discharge area for the unconfined aquifer system was approximated  
28 in the three-dimensional model with a constant-head boundary applied at the uppermost nodes of the  
29 model at the approximate locations of the river's left bank and channel midpoint. Nodes representing the  
30 thickness of the aquifer below the nodes representing mid-point of the river channel were treated as  
31 no-flow boundaries. This boundary condition is used to approximate the location of the groundwater  
32 divide that exists beneath the Columbia River where groundwater from the Hanford Site and the other  
33 side of the river discharge into the Columbia. The long-term, average river-stage elevations for the  
34 Columbia River implemented in the sitewide model were based on results from previous work performed  
35 by Walters et al. (1994) for the Columbia River with the CHARIMA river simulation model. The  
36 Yakima River was also represented as a specified-head boundary at surface nodes approximating its  
37 location. Like the Columbia River, nodes representing the thickness of the aquifer below the Yakima  
38 River channel were treated as no-flow boundaries. Short-term fluctuations in the river levels do not  
39 influence modeling results.  
40

41 At Cold Creek and Dry Creek Valleys, the unconfined aquifer system extends westward beyond the  
42 boundary of the model. To approximate the groundwater flux entering the modeled area from these  
43 valleys, both constant-head and constant-flux boundary conditions were defined. A constant-head  
44 boundary condition was specified for Cold Creek Valley for the steady-state model calibration runs. The



pdt99012.eps

1  
2  
3 **Figure G.6.** Peripheral Boundaries Defined for the Three-Dimensional Model (taken from  
4 Cole et al. (1997))  
5

6 fluxes resulting from the specified-head boundaries in the calibrated steady-state model were then used in  
7 the steady-state flow simulation of flow conditions after Hanford Site closure. The constant-flux  
8 boundary was used because it better represents the response of the boundary to a declining water table

1 than does a constant-head boundary. Discharges from Dry Creek Valley in the model area, resulting from  
2 infiltration of precipitation and spring discharges, are approximated using the same methods.

3  
4 The basalt underlying the unconfined aquifer sediments represents a lower boundary to the  
5 unconfined aquifer system. The potential for interflow (recharge and discharge) between the basalt-  
6 confined aquifer system and the unconfined aquifer system is largely unquantified but is postulated to be  
7 small relative to the other flow components estimated for the unconfined aquifer system. Therefore,  
8 interflow with underlying basalt units was not included in the current three-dimensional model. The  
9 basalt was defined in the model as an essentially impermeable unit underlying the sediments.

### 10 11 **G.1.5.1.3 Flow and Transport Properties**

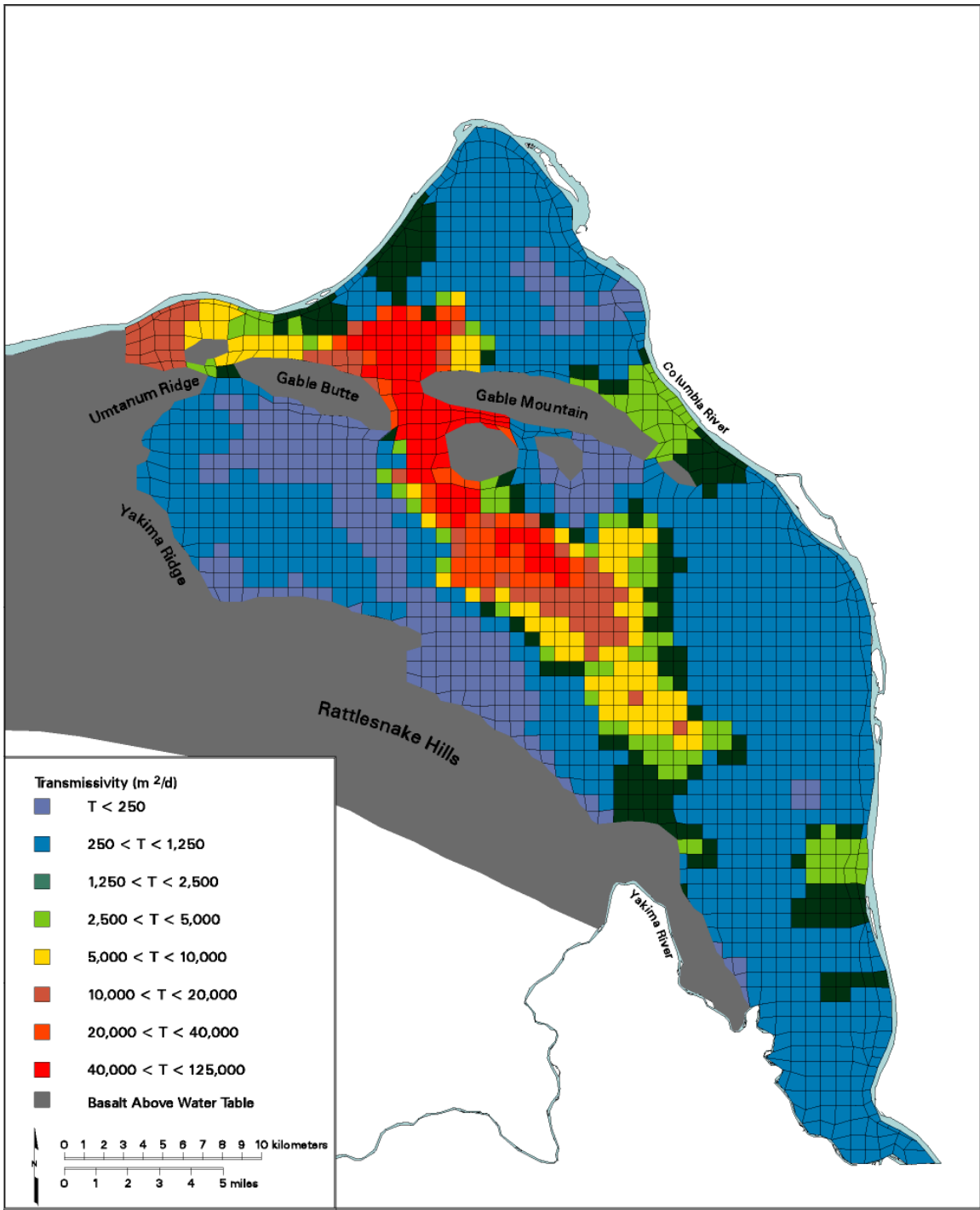
12  
13 To model groundwater flow, the distribution of hydraulic properties, including horizontal and vertical  
14 hydraulic conductivity, storativity, and specific yield, was needed for each hydrogeologic unit defined in  
15 the model. In addition, to simulate movement of contaminant plumes, transport properties were needed,  
16 including contaminant-specific distribution coefficients, bulk density, effective porosity, and longitudinal  
17 and transverse dispersivities.

18  
19 In the original model calibration procedure described in Wurstner et al. (1995), measured values of  
20 aquifer transmissivity were used in a two-dimensional model with an inverse model-calibration procedure  
21 to determine the transmissivity distribution. Hydraulic head conditions for 1979 were used in the inverse  
22 calibration because measured hydraulic heads were relatively stable at that time. Details concerning the  
23 updated calibration of the two-dimensional model are provided in Cole et al. (1997). The resulting  
24 transmissivity distribution for the unconfined aquifer system is shown in Figure G.10.

25  
26 Hydraulic conductivities were assigned to the three-dimensional model units so that the total aquifer  
27 transmissivity from inverse calibration was preserved at every location. The vertical distribution of  
28 hydraulic conductivity at each spatial location was determined, based on the transmissivity value and  
29 other information, including facies descriptions and hydraulic property values measured for similar facies.  
30 A complete description of the seven-step process used to vertically distribute the transmissivity among the  
31 model hydrogeologic units is described in Cole et al. (1997).

32  
33 The current version of the sitewide model relies on a three-dimensional representation of the aquifer  
34 system that was calibrated to Hanford Sitewide groundwater monitoring data collected during Hanford  
35 operations from 1943 to the present. The calibration procedure and results for this model are described in  
36 Cole et al. (2001a). This recent work is part of a broader effort to develop and implement a stochastic  
37 uncertainty estimation methodology in future assessments and analyses using the sitewide groundwater  
38 model (Cole et al. 2001b). Resulting distribution of hydraulic conductivities from this recent calibration  
39 effort is provided in Figures G.8 and G.9.

40  
41 Information on transport properties used in past modeling studies at the Hanford Site is provided in  
42 Wurstner et al. (1995). Estimates of model parameters were developed to account for contaminant  
43 dispersion and adsorption in all transport simulations. Specific model parameters examined included  
44 longitudinal and transverse dispersivity ( $D_L$  and  $D_T$ ) and contaminant retardation factors ( $R_d$ ). Calculation

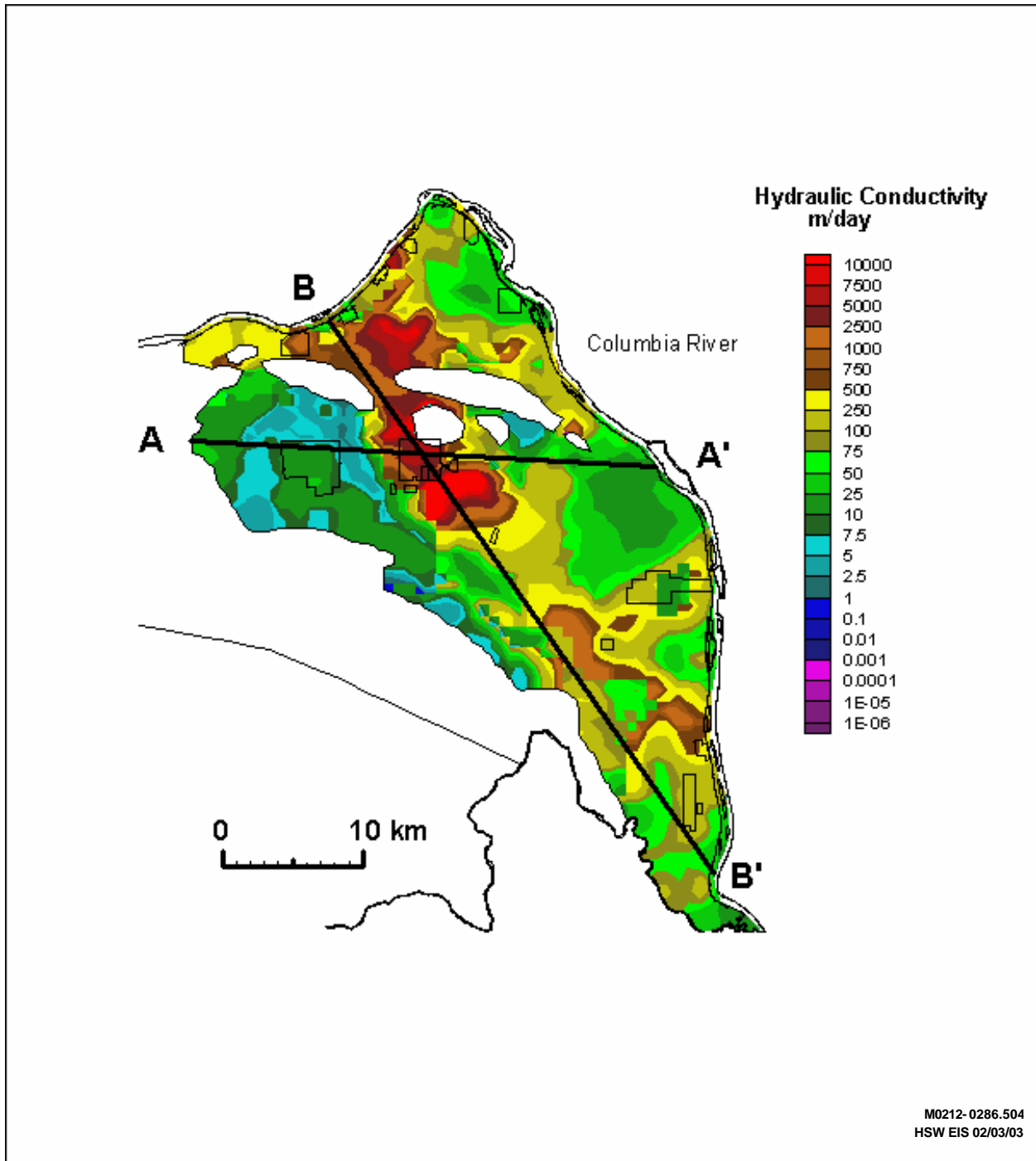


skw99002.apr January 25, 1999

M0212-0286.69  
HSW EIS 12/10/02

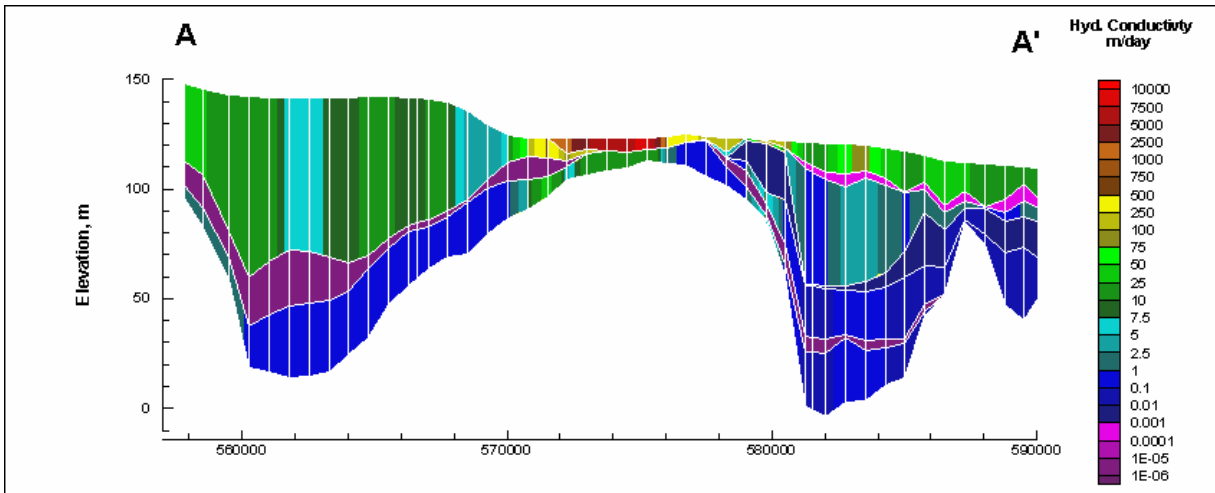
**Figure G.7.** Transmissivity Distribution for the Unconfined Aquifer System Based on Two-Dimensional Inverse Model Calibration (after Wurstner et al. 1995)

1  
2  
3  
4  
5

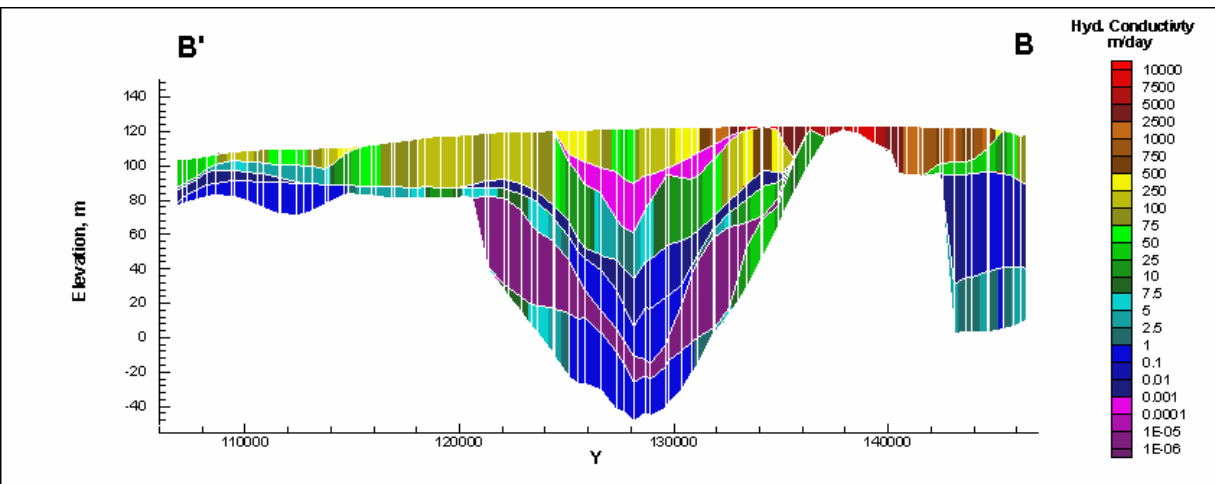


1  
2  
3  
4  
5

**Figure G.8.** Distribution of Estimated Hydraulic Conductivities at Water Table from Best-Fit Inverse Calibration of Sitewide Groundwater Model by Cole et al. (2001a)



1  
2



3  
4

M0212-0286.505  
HSW EIS 02/03/03

5  
6

**Figure G.9.** Distribution of Estimated Hydraulic Conductivities Along Section Lines A-A' and B-B' from Best-Fit Inverse Calibration of Sitewide Groundwater Model by Cole et al. (2001a)

7  
8

of effective  $R_f$  required estimates of contaminant-specific distribution coefficients, as well as estimates of effective bulk density and porosity of the aquifer materials. The remainder of this section briefly summarizes estimated transport properties.

9  
10  
11  
12

For this analysis, a longitudinal dispersivity,  $D_L$ , of a little less than 100 m (95 m) (310 ft) was selected using this typical approach for estimating longitudinal dispersivity based on the scale of interest. Although transport results produced in this analysis span a range of scales, the key scale of interest is the minimum distance between some of the source areas in the Central Plateau and the location of the buffer zone boundary surrounding this area. For some sources in 200 East Area, the distance of interest is on the order of 1 to 2 kilometers away. Thus, a dispersivity value used in the original analysis was selected to be approximately equal to 10 percent of the minimum travel distance of interest of about 1 km (0.6 mi).

13  
14  
15  
16  
17  
18  
19  
20

1 The longitudinal dispersivity was also consistent to be within the range of recommended grid Peclet  
2 numbers ( $Pe < 4$ ) for acceptable solutions. The 95-m (310-ft) estimate is about one-quarter of the grid  
3 spacing in the finest part of the model grid in the Central Plateau where the smallest grid spacing is about  
4 375 m by 375 m (1230 ft x 1230 ft).

5  
6 The corresponding transverse dispersivity used in the analysis was selected to be consistent with  
7 general available regulatory and technical guidance. EPA guidance (Mills et al. 1985) on the subject  
8 suggests a 1 to 3 ratio for  $D_T$  to  $D_L$ . Freeze and Cherry (1979) report that transverse dispersivities used  
9 are normally lower than the longitudinal dispersivity by a factor of 5 to 20 (that is, 0.2 to 0.05). Walton  
10 (1985) states that reported ratios of  $D_T$  to  $D_L$  vary from 1 to 24 but that common values are 0.2 and 0.1.  
11 Considering this information, a transverse dispersivity,  $D_T$ , used in Composite Aanalysis simulations was  
12 assumed to be about 20 m (65.6 ft), which is approximately 20 percent of the selected longitudinal  
13 dispersivity.

14  
15 The longitudinal dispersivity was also consistent and within the range of recommended grid Peclet  
16 numbers ( $Pe < 4$ ) for acceptable solutions. The 95-m (310-ft) estimate is about one-quarter of the grid  
17 spacing in the finest part of the model grid in the Central Plateau where the smallest grid spacing is about  
18 375 m by 375 m (1230 ft x 1230 ft).

19  
20 In addition to the estimated distribution coefficient, calculation of contaminant-specific retardation  
21 factors used in the model requires estimates of the effective bulk density and porosity. For purposes of  
22 these calculations, a bulk density of  $1.9 \text{ g/cm}^3$  was used for all simulations. The effective porosity was  
23 estimated from specific yields obtained from multiple well aquifer tests. These values range from 0.01 to  
24 0.37. Laboratory measurements of porosity that range from 0.19 to 0.41 were available for samples from  
25 a few Hanford Site wells and were also considered. The few tracer tests conducted indicate effective  
26 porosities ranging from 0.1 to 0.25. Within the model, a porosity value of 0.1 was used for the Ringold  
27 Formation (Model Units 4 through 9) and a porosity value of 0.25 was used for the Hanford formation  
28 (Model Unit 1). For the expected lower water table conditions during the post-Hanford period, the Early  
29 Palouse and Plio-Pleistocene hydrogeologic units (Model Units 2 and 3) only existed above the projected  
30 water table and were not considered in the analysis. Values of distribution coefficient, bulk density,  
31 effective porosity, and dispersivity used in this analysis are discussed in more detail in Cole et al. (1997).

### 32 33 **G.1.5.2 Simulation of Post-Closure Flow Conditions**

34  
35 Past projections of water table conditions after site closure have estimated the impact of Hanford  
36 operations ceasing and the resulting changes in artificial discharges that have been used extensively as a  
37 part of site waste management practices. Simulations of transient-flow conditions from 1944 through the  
38 year 3050 were conducted by Bryce et al. (2002). The three-dimensional model shows an overall decline  
39 in the hydraulic head and hydraulic gradient across the entire water table within the modeled region.  
40 Results of these simulations suggest that the water table would reach steady state between 100 to  
41 350 years in different areas over the Hanford Site. These results were generally consistent with findings  
42 for the similar conditions in earlier modeling by Cole et al. (1997) and Kincaid et al. (1998).

1 Given the expected long delay of contaminants reaching the water from the LLBGs, the hydrologic  
2 framework of all groundwater transport calculations was based on postulated post-Hanford steady-state  
3 water table as estimated with the three-dimensional model. These conditions would only reflect estimated  
4 boundary condition fluxes (for example, natural recharge and lateral boundary fluxes) and not the effect  
5 of past and current wastewater discharges on the unconfined aquifer system.  
6

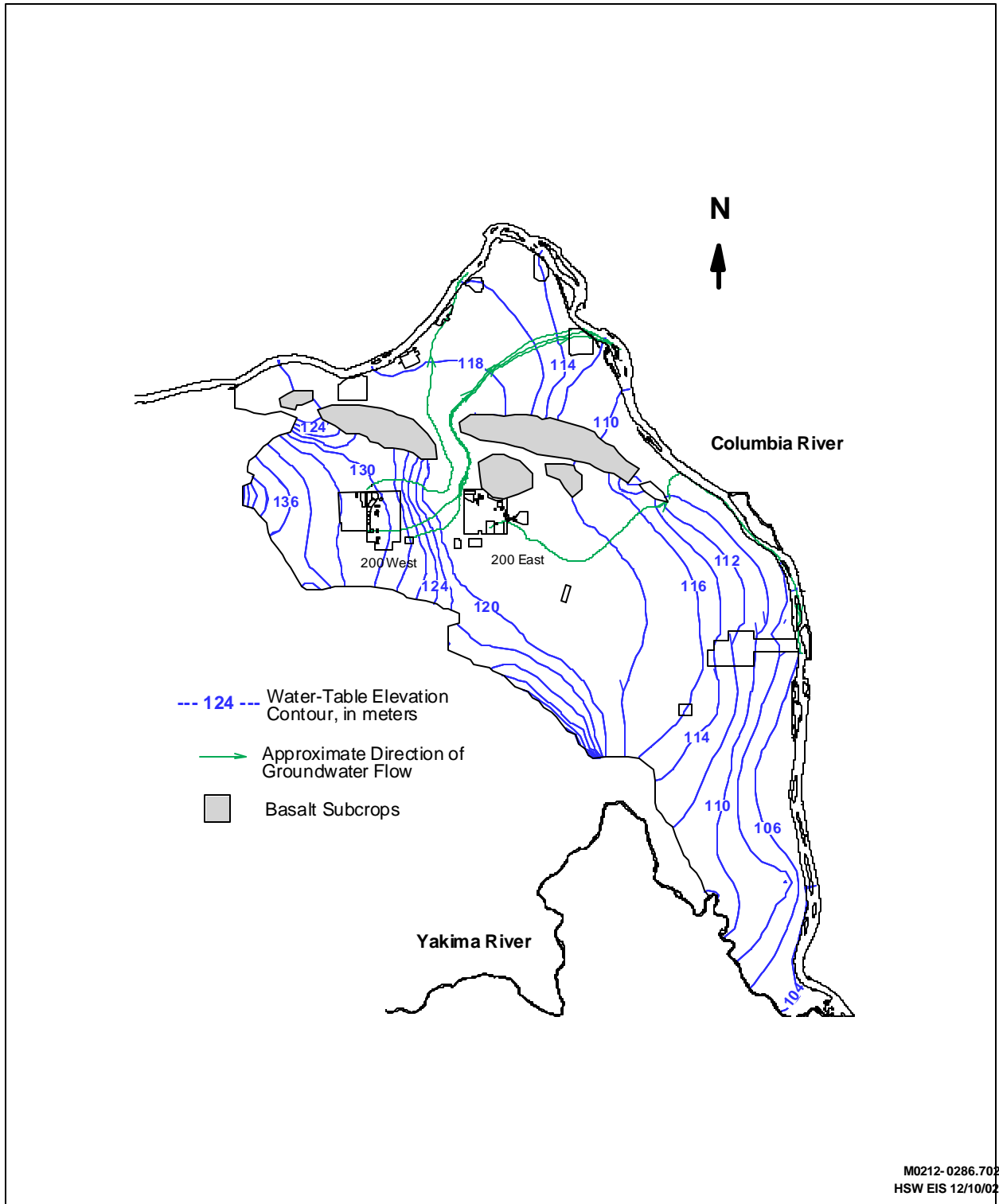
7 Flow modeling results also suggest that as water levels drop in the vicinity of central areas in the  
8 model where the basalt crops out above the water table, the saturated thickness of the unconfined aquifer  
9 will decrease and the aquifer may actually dry out in certain areas. This thinning/drying of the aquifer is  
10 predicted to occur in the area just north of the 200 East Area between Gable Butte and the outcrop south  
11 of Gable Mountain, and there is the potential of this northern area of the unconfined aquifer becoming  
12 hydrologically separated from the area south of Gable Mountain and Gable Butte. Because of the  
13 uncertainty in the potential natural recharge and boundary fluxes from up-gradient areas, the potential for  
14 movement of contaminants either through the gap or to the east toward the Columbia River is also  
15 uncertain. To address this uncertainty, two predicted water tables for these post-Hanford steady-state  
16 conditions, as illustrated in Figures G.10 and G.11, were considered.  
17

18 The first scenario, shown in Figure G.10, estimates flow conditions where basalt sub-crops estimated  
19 to be above the water table north of the Central Plateau are consistent with those used in the most recent  
20 assessments by Bryce et al. (2002). Under this scenario, the overall flow attributes of the water table  
21 surface lead to groundwater flow and transport through the gap between Gable Mountain and Gable Butte  
22 from most areas in the 200 East and 200 West Areas. This scenario was the flow condition used in all  
23 groundwater flow and transport calculations presented in the following sections.  
24

25 In the second scenario, shown in Figure G.11, flow conditions are reflective of assumed basalt sub-  
26 crops just north of the 200 East Area that are more widespread and effectively cut off the flow and  
27 transport from both the 200 East and 200 West Areas to the north through the gap between Gable  
28 Mountain and Gable Butte. The overall flow attributes of this water table surface leads to a predominant  
29 easterly flow direction from nearly all areas within the 200 East and 200 West Areas. The effect of this  
30 scenario on calculated results, while not considered in all results presented in Section G.2, is briefly  
31 discussed in the following section and in a discussion of results for Alternative Group A in Section G.2.1.  
32

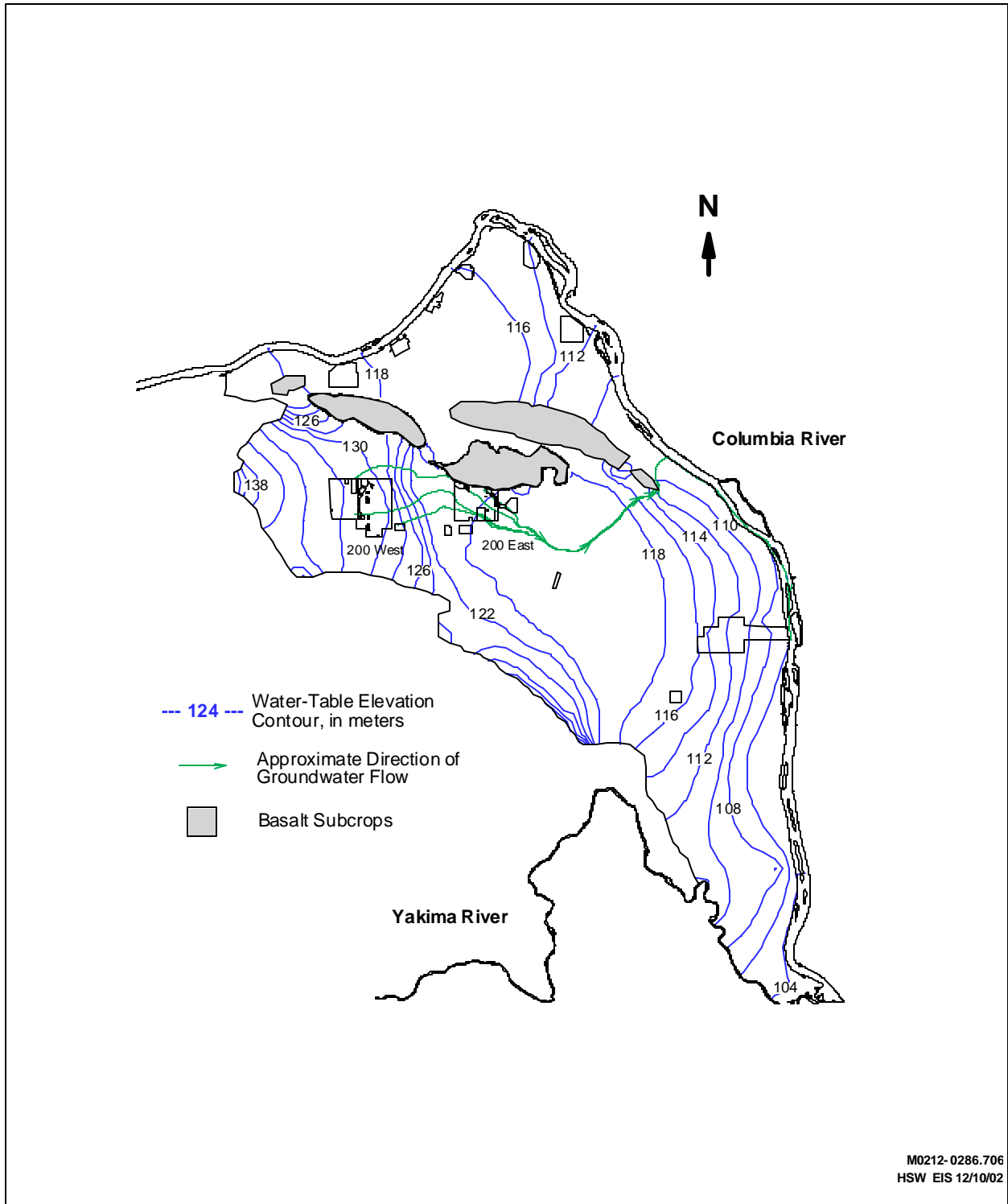
### 33 **G.1.5.3 Simulation of Unit Releases** 34

35 To allow groundwater transport calculations to be used in the convolution approach for linear  
36 superposition (See Section G.1.2), a unit release was simulated with the three-dimensional model and the  
37 estimated post-Hanford steady-state water table condition. These simulation results are used to relate the  
38 effect of known release (1 curie over a 10-year period) to predicted concentrations at various points in the  
39 aquifer system. Example results of simulated groundwater concentrations in response to a unit release of  
40 a long-lived, mobile (non-sorbing) contaminant over a period of 10 years from MLLW disposal sites in  
41 the 200 West and 200 East Areas are illustrated in Figures G.15 and G.16, respectively. These  
42 simulations were made using the groundwater conceptual model with a predominant northerly flow  
43 pattern out of the Central Plateau.



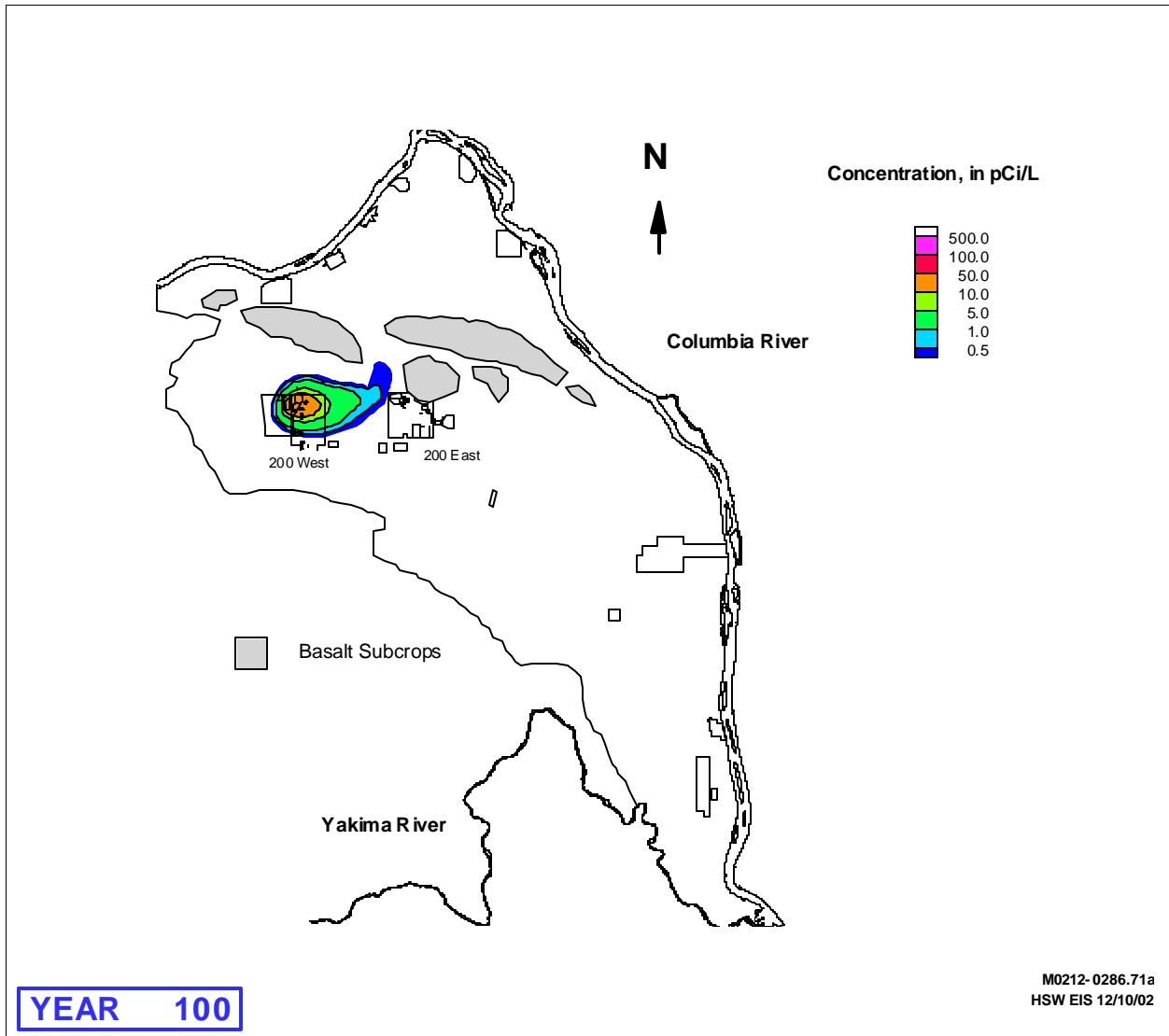
1  
2  
3

**Figure G.10.** Predicted Post-Hanford Water Table Conditions (Predominant Northerly Flow)



1  
2  
3

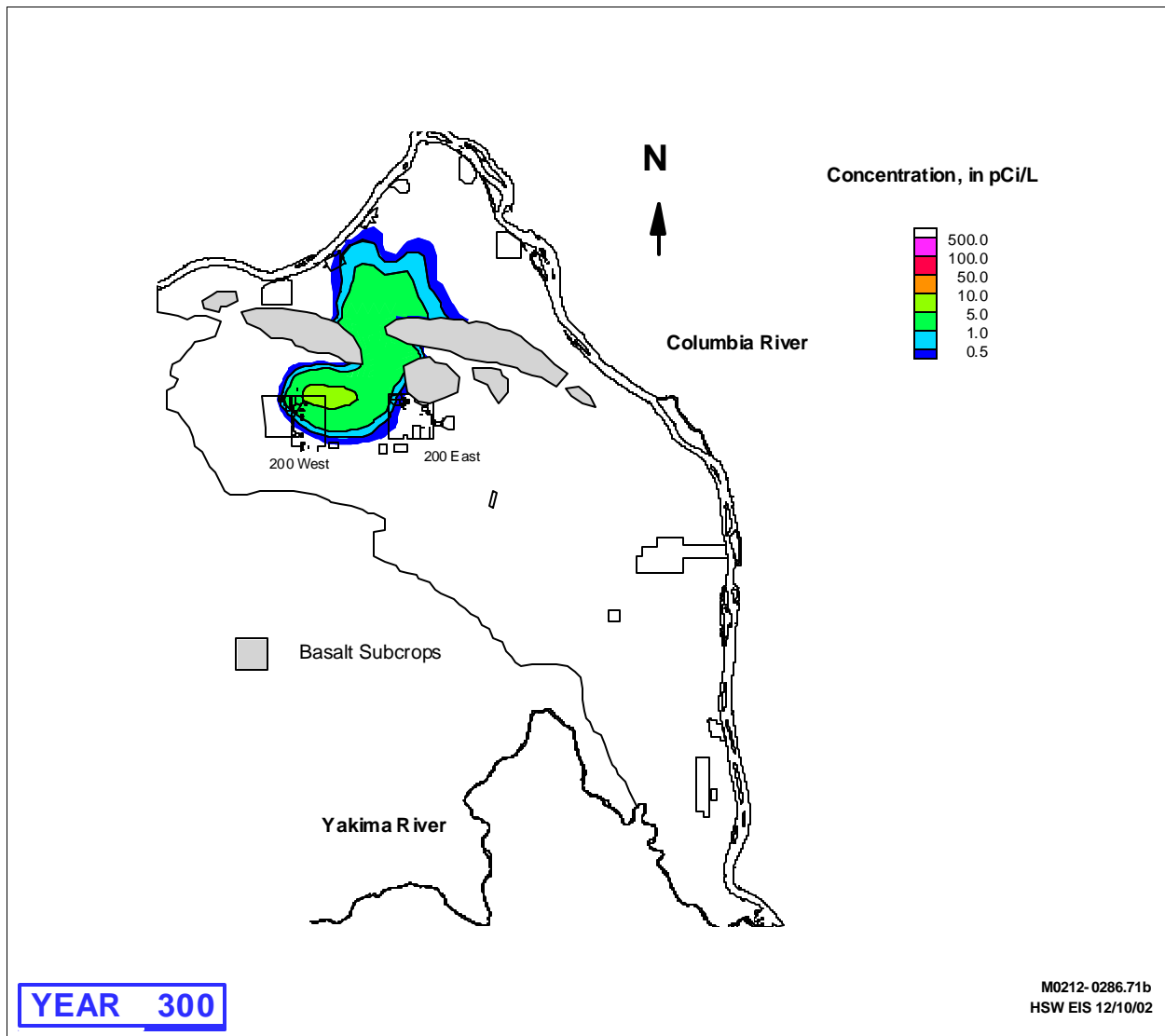
**Figure G.11.** Predicted Post-Hanford Water Table Conditions (Predominant Easterly Flow)



1  
2  
3  
4  
5

**Figure G.12a.** Simulated Transport of a 10-Year Unit Release (1 Curie) of a Contaminant Representative of Mobility Class 1<sup>(a)</sup> from MLLW in the 200 West Area at 100 Years After Release Using a Groundwater Model with a Predominant Northerly Flow from the Central Plateau

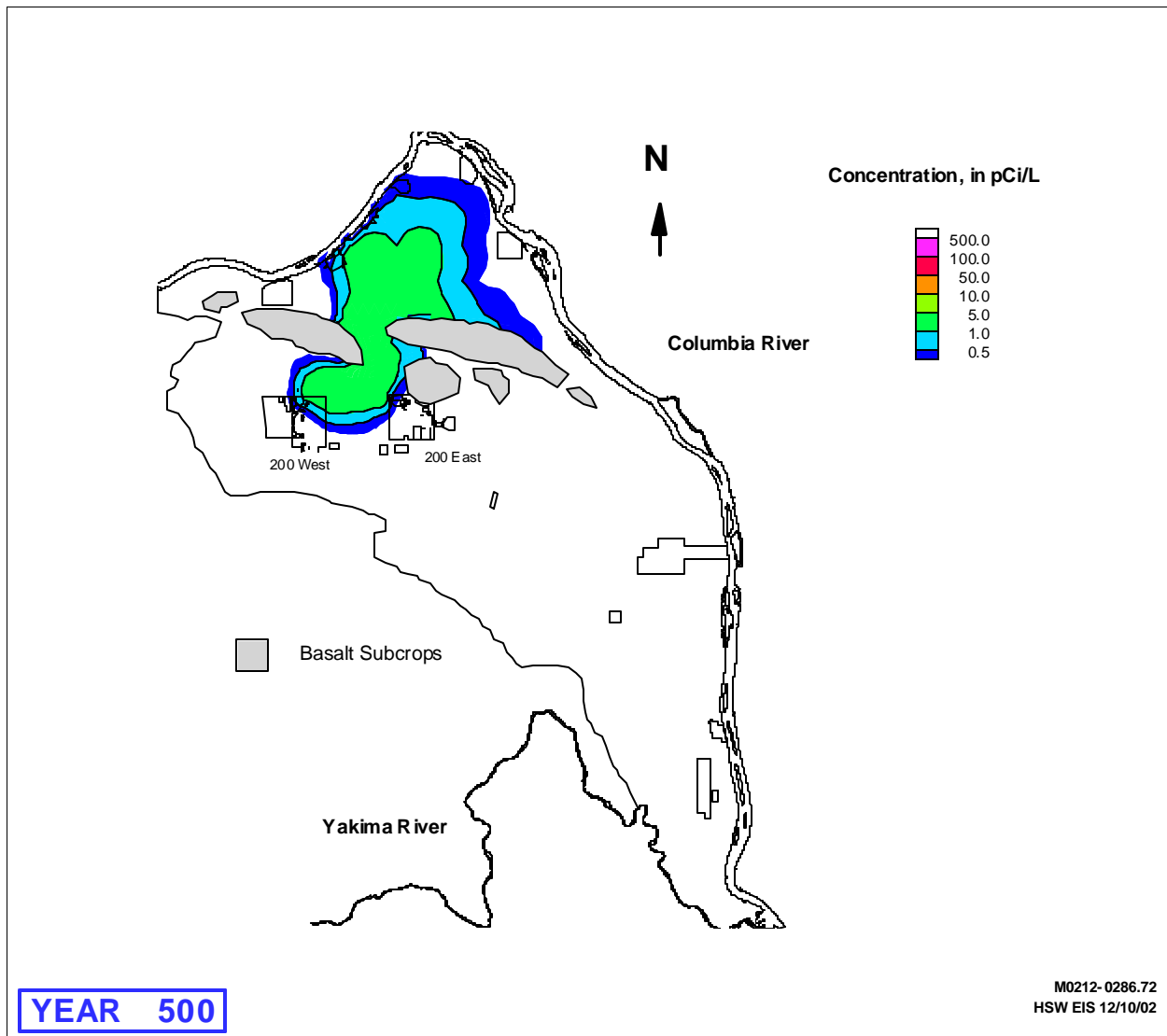
(a) These simulation results relate the effect of a known release (1 curie over a period of 10 years) of a hypothetical, long-lived contaminant in Mobility Class 1 to predicted concentrations at various points in the aquifer system. These results provide the basis for the groundwater transport component of the convolution approach described in Section G.1.2.



1  
2  
3  
4  
5

**Figure G.12b.** Simulated Transport of a 10-Year Unit Release (1 Curie) of a Contaminant Representative of Mobility Class 1<sup>(a)</sup> from MLLW in the 200 West Area at 300 Years After Release Using a Groundwater Model with a Predominant Northerly Flow from the Central Plateau

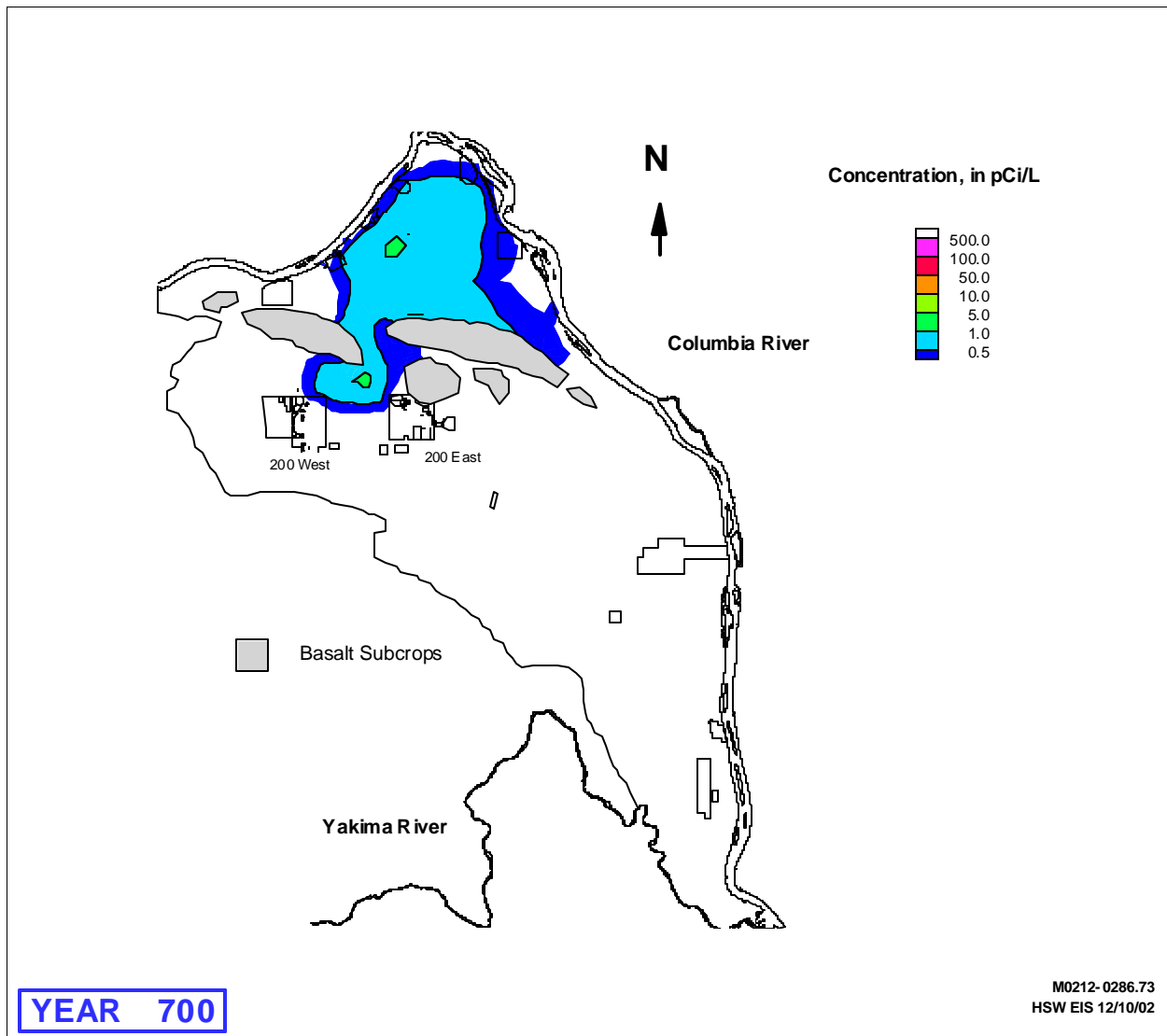
(a) These simulation results relate the effect of a known release (1 curie over a period of 10 years) of a hypothetical, long-lived contaminant in Mobility Class 1 to predicted concentrations at various points in the aquifer system. of an unretarded long-lived contaminant. These results provide the basis for the groundwater transport component of the convolution approach described in Section G.1.2.



1  
2  
3  
4  
5  
6

**Figure G.12c.** Simulated Transport of a 10-Year Unit Release (1 Curie) of a Contaminant Representative of Mobility Class 1<sup>(a)</sup> from MLLW in the 200 West Area at 500 Years After Release Using a Groundwater Model with a Predominant Northerly Flow from the Central Plateau

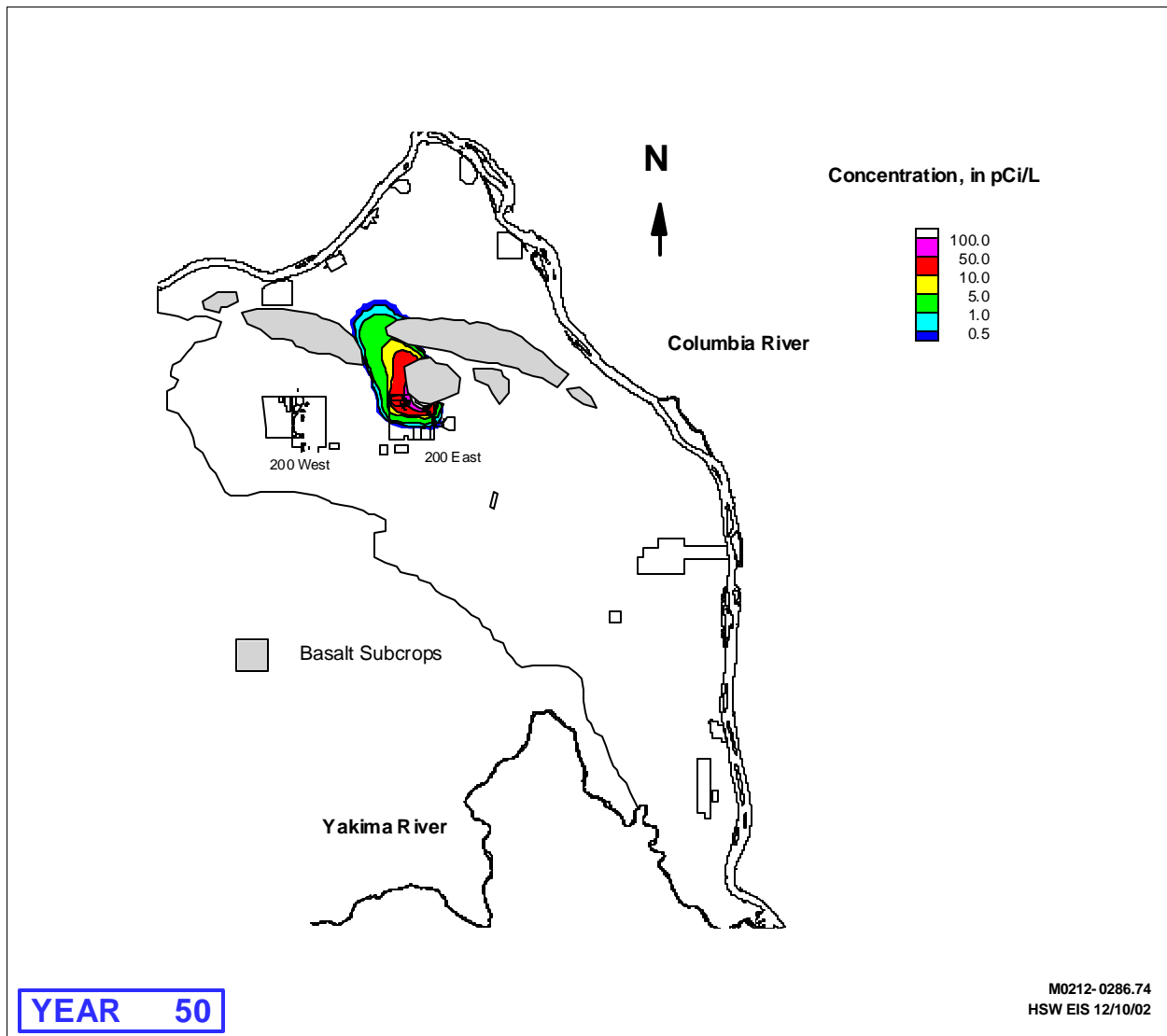
(a) These simulation results relate the effect of a known release (1 curie over a period of 10 years) of a hypothetical, long-lived contaminant in Mobility Class 1 to predicted concentrations at various points in the aquifer system. These results provide the basis for the groundwater transport component of the convolution approach described in Section G.1.2.



1  
2  
3  
4  
5

**Figure G.12d.** Simulated Transport of a 10-Year Unit Release (1 Curie) of a Contaminant Representative of Mobility Class 1<sup>(a)</sup> from MLLW in the 200 West Area at 700 Years After Release Using a Groundwater Model with a Predominant Northerly Flow from the Central Plateau

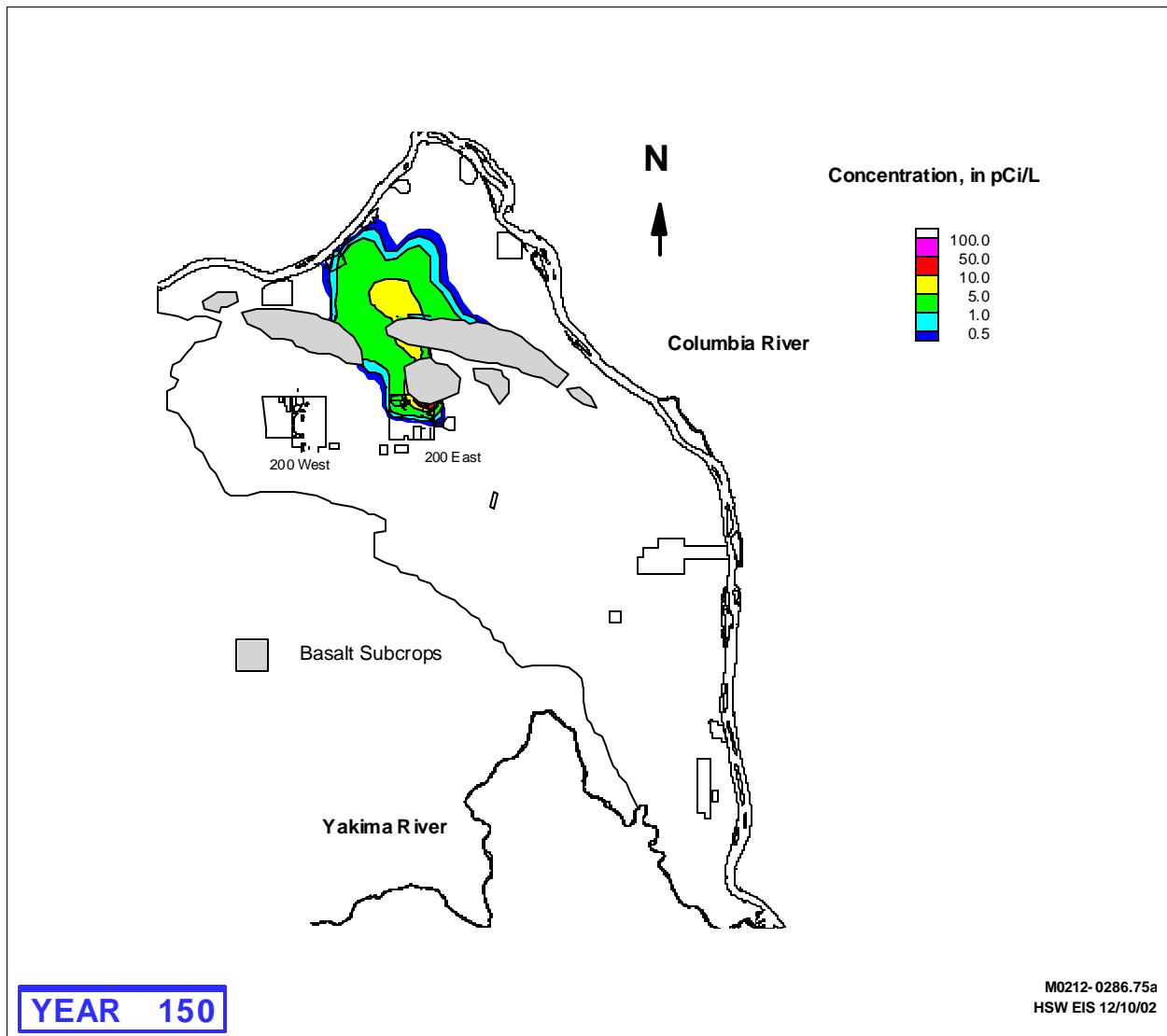
(a) These simulation results relate the effect of a known release (1 curie over a period of 10 years) of a hypothetical, long-lived contaminant in Mobility Class 1 to predicted concentrations at various points in the aquifer system. These results provide the basis for the groundwater transport component of the convolution approach described in Section G.1.2.



1  
2  
3  
4  
5

**Figure G.13a.** Simulated Transport of a 10-Year Unit Release (1 Curie) of a Contaminant Representative of Mobility Class 1<sup>(a)</sup> from MLLW in the 200 East Area at 50 Years After Release Using a Groundwater Model with a Predominant Northerly Flow from the Central Plateau

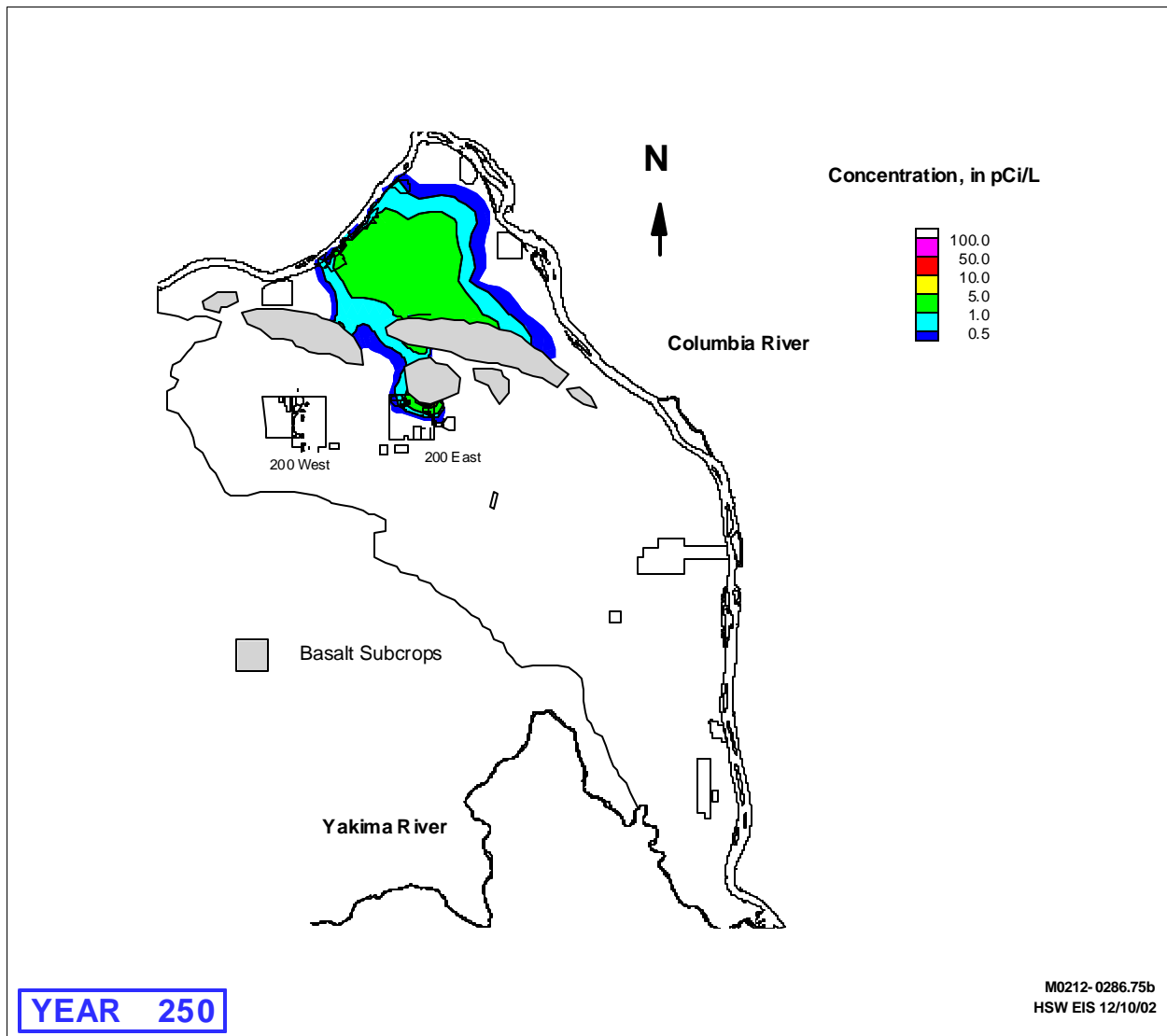
(a) These simulation results relate the effect of a known release (1 curie over a period of 10 years) of a hypothetical, long-lived contaminant in Mobility Class 1 to predicted concentrations at various points in the aquifer system. These results provide the basis for the groundwater transport component of the convolution approach described in Section G.1.2.



1  
2  
3  
4  
5

**Figure G.13b.** Simulated Transport of a 10-Year Unit Release (1 Curie) of a Contaminant Representative of Mobility Class 1<sup>(a)</sup> from MLLW in the 200 East Area at 150 Years After Release Using a Groundwater Model with a Predominant Northerly Flow from the Central Plateau

(a) These simulation results relate the effect of a known release (1 curie over a period of 10 years) of a hypothetical, long-lived contaminant in Mobility Class 1 to predicted concentrations at various points in the aquifer system. These results provide the basis for the groundwater transport component of the convolution approach described in Section G.1.2.



1  
2  
3  
4  
5  
6

**Figure G.13c.** Simulated Transport of a 10-Year Unit Release (1 Curie) of of a Contaminant Representative of Group 1<sup>(a)</sup> from MLLW in the 200 East Area at 250 Years After Release Using a Groundwater Model with a Predominant Northerly Flow from the Central Plateau

(a) These simulation results relate the effect of a known release (1 curie over a period of 10 years) of a hypothetical, long-lived contaminant in Mobility Class 1 to predicted concentrations at various points in the aquifer system. These results provide the basis for the groundwater transport component of the convolution approach described in Section G.1.2.

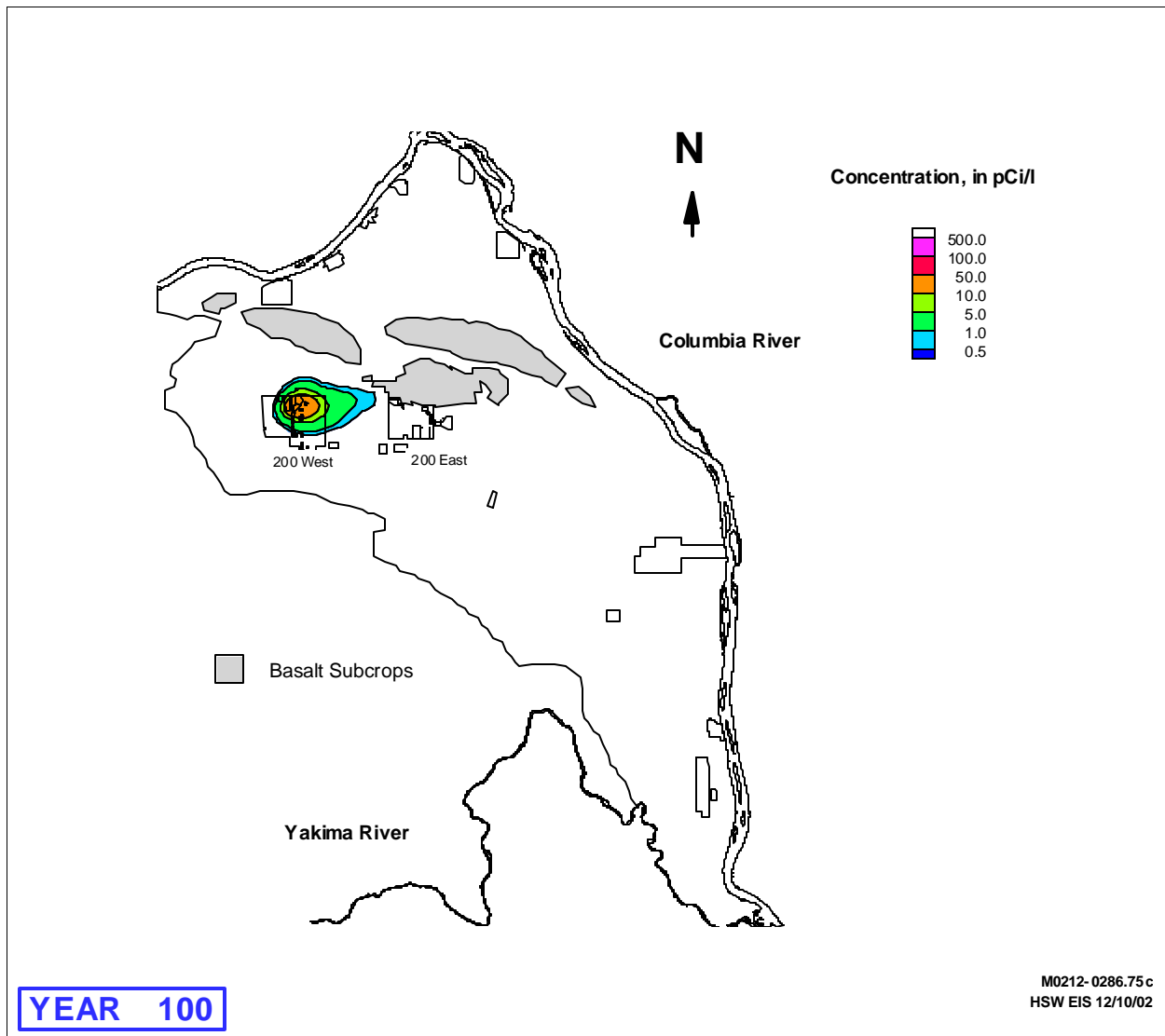
1 The same calculations were also made using the alternative groundwater conceptual model with  
2 easterly flow from the 200 East Area. Results of this model at the same MLLW disposal locations in the  
3 200 West and East Areas are illustrated in Figures G.14 and G.15, respectively.  
4

5 Results of these unit releases were evaluated to identify the maximum concentrations over time for  
6 use in the convolution approach along the LOAs down-gradient of the 200 East and West Areas and  
7 ERDF HSW disposal areas (See Figure G.6) as appropriate for each alternative group. Because the  
8 location of different waste categories within each of the aggregate HSW disposal areas varies as specified  
9 for each alternative group, the locations of maximum concentration along the LOAs may not necessarily  
10 correspond to the same location for each waste category specified within and across alternative groups.  
11 This is particularly true for breakthrough curves developed for LOAs along the Columbia River where the  
12 location of maximum concentration varies in time as the simulated plumes migrate north to the Columbia  
13 River. The specific calculations presented here were used to evaluate groundwater transport of  
14 contaminants in Group 1 (technetium-99 and iodine-129). Similar calculations were made to evaluate  
15 groundwater transport of the same Group 1 contaminants and for contaminants in Group 2 (carbon-14 and  
16 uranium isotopes) for other waste category locations in the overall convolution approach.  
17

18 A comparison of unit release breakthrough curves for Group 1 constituents at the 200 East and West  
19 Area, ERDF, and Columbia River LOAs for the two alternative groundwater conceptual models are  
20 presented in a series of plots in Figures 16 and 17 for all waste categories to illustrate differences in  
21 results for the two groundwater conceptual models. Under the first alternative model, impacts from LLW  
22 disposed of in the 200 East Area LLBGs are evaluated at the 200 East Area NW LOA. Impacts from  
23 LLW disposed of near the PUREX Plant are evaluated at the 200 East Area SE LOA. Under the second  
24 alternative, where groundwater flow is toward the east from the 200 Areas, impacts from LLW disposed  
25 of in the 200 East Area LLBGs or near the PUREX Plant are evaluated at the 200 East Area SE LOA.  
26

27 Results of these calculations show very little change in breakthrough curves calculated from  
28 200 West Area and ERDF sources in both models. Peak concentrations of long-lived mobile contami-  
29 nants (like technetium-99 or iodine-129) released in the 200 West Area and the ERDF would reach the  
30 1-km (0.6-mi) LOAs between 80 and 200 years. Times of peak concentration at the Columbia River in  
31 areas north through the gap between Gable Mountain and Gable Butte using the first groundwater con-  
32 ceptual model between 400 and 500 years for sources in the 200 West Area and about 300 years from  
33 sources at the ERDF. Concentration levels of the river are slightly lower for the second alternative  
34 model. This is consistent with the general plume migration behavior in the second alternative model  
35 since a secondary part of plume splits off of the main lobe originating from the 200 West Area and  
36 migrates to the east across the 200 East Area, where it eventually discharges into the Columbia River near  
37 the Hanford town site.  
38

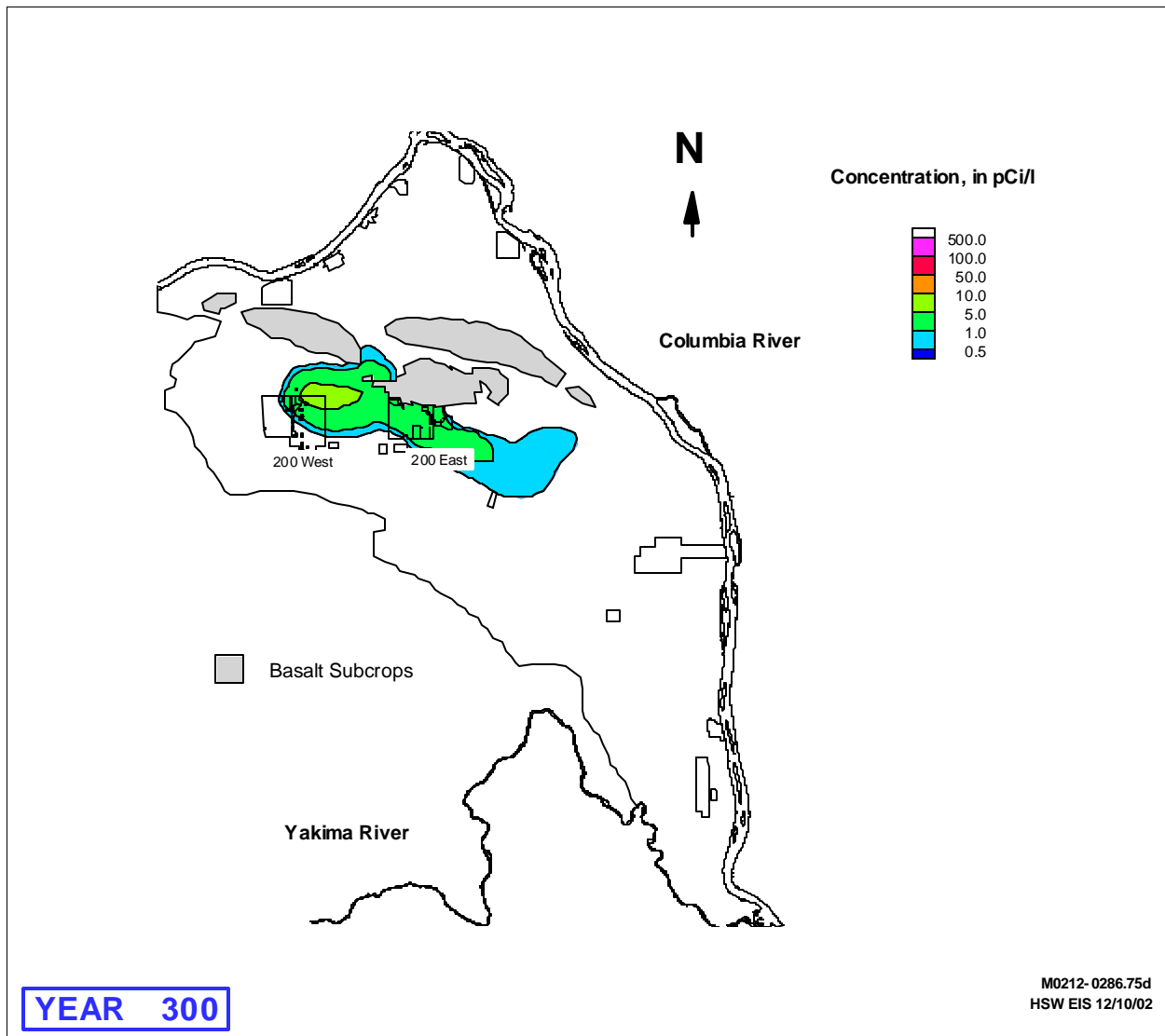
39 Peak concentrations of mobile contaminants introduced at the water table beneath HSW disposal sites  
40 in the 200 East Area would reach the 1-km (0.6-mi) LOAs within 30 to 50 years and migrate only about  
41 150 to 250 years before reaching the Columbia River north through the gap in the first groundwater  
42 model. In the second alternative model, arrival at the 1 km (0.6 mi) LOA is very rapid—within  
43 10 years—and reaches the Columbia River near the Hanford town site within 100 years.



1  
2  
3  
4  
5

**Figure G.14a.** Simulated Transport of a 10-Year Unit Release (1 Curie) of a Contaminant Representative of Mobility Class 1<sup>(a)</sup> from MLLW in the 200 West Area at 100 Years After Release Using a Groundwater Model with a Predominant Easterly Flow from the Central Plateau

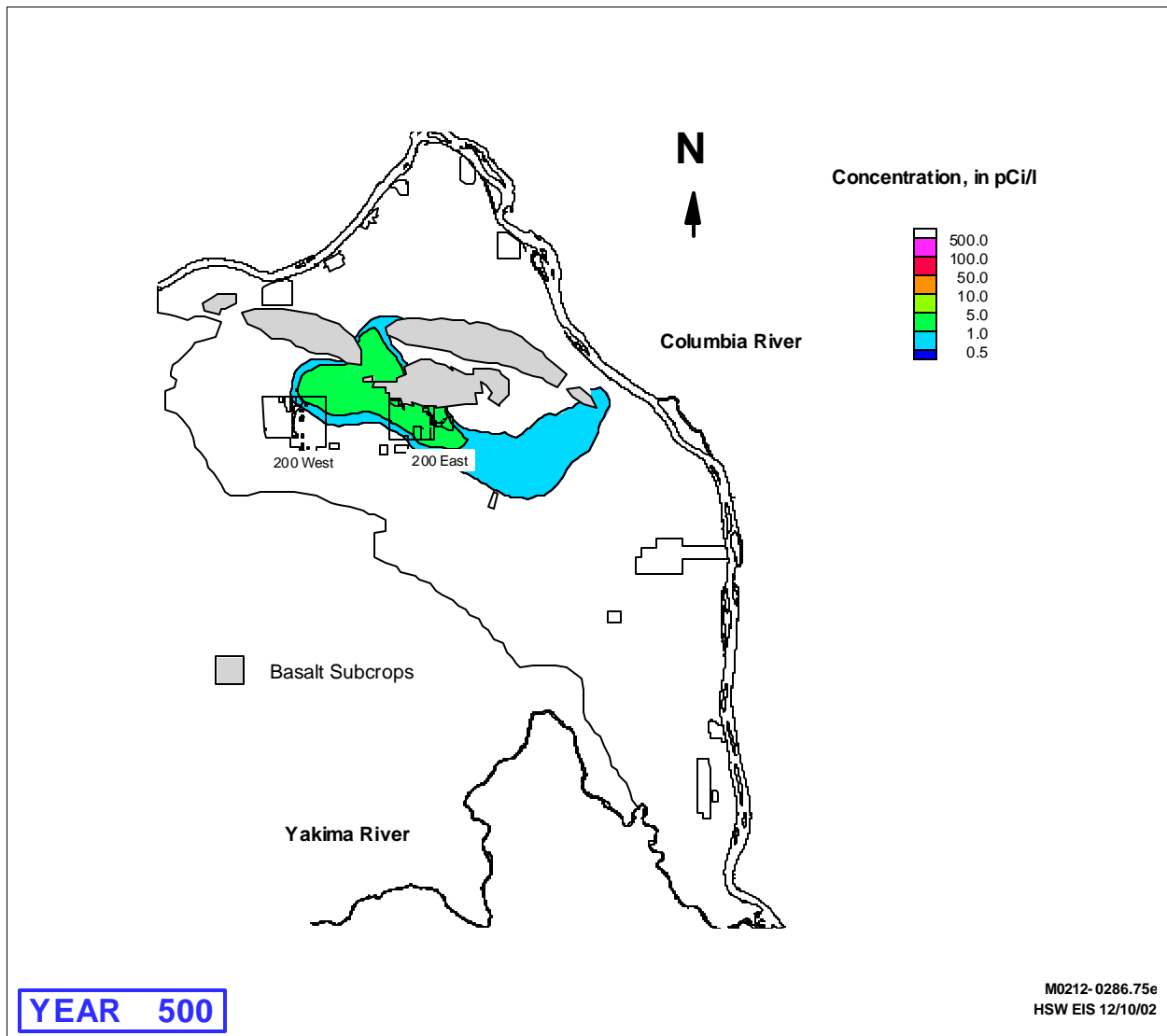
(a) These simulation results relate the effect of a known release (1 curie over a period of 10 years) of a hypothetical, long-lived contaminant in Mobility Class 1 to predicted concentrations at various points in the aquifer system. These results provide the basis for the groundwater transport component of the convolution approach described in Section G.1.2.



1  
2  
3  
4  
5

**Figure G.14b.** Simulated Transport of a 10-Year Unit Release (1 Curie) of a Contaminant Representative of Mobility Class 1<sup>(a)</sup> from MLLW in the 200 West Area at 300 Years After Release Using a Groundwater Model with a Predominant Easterly Flow from the Central Plateau

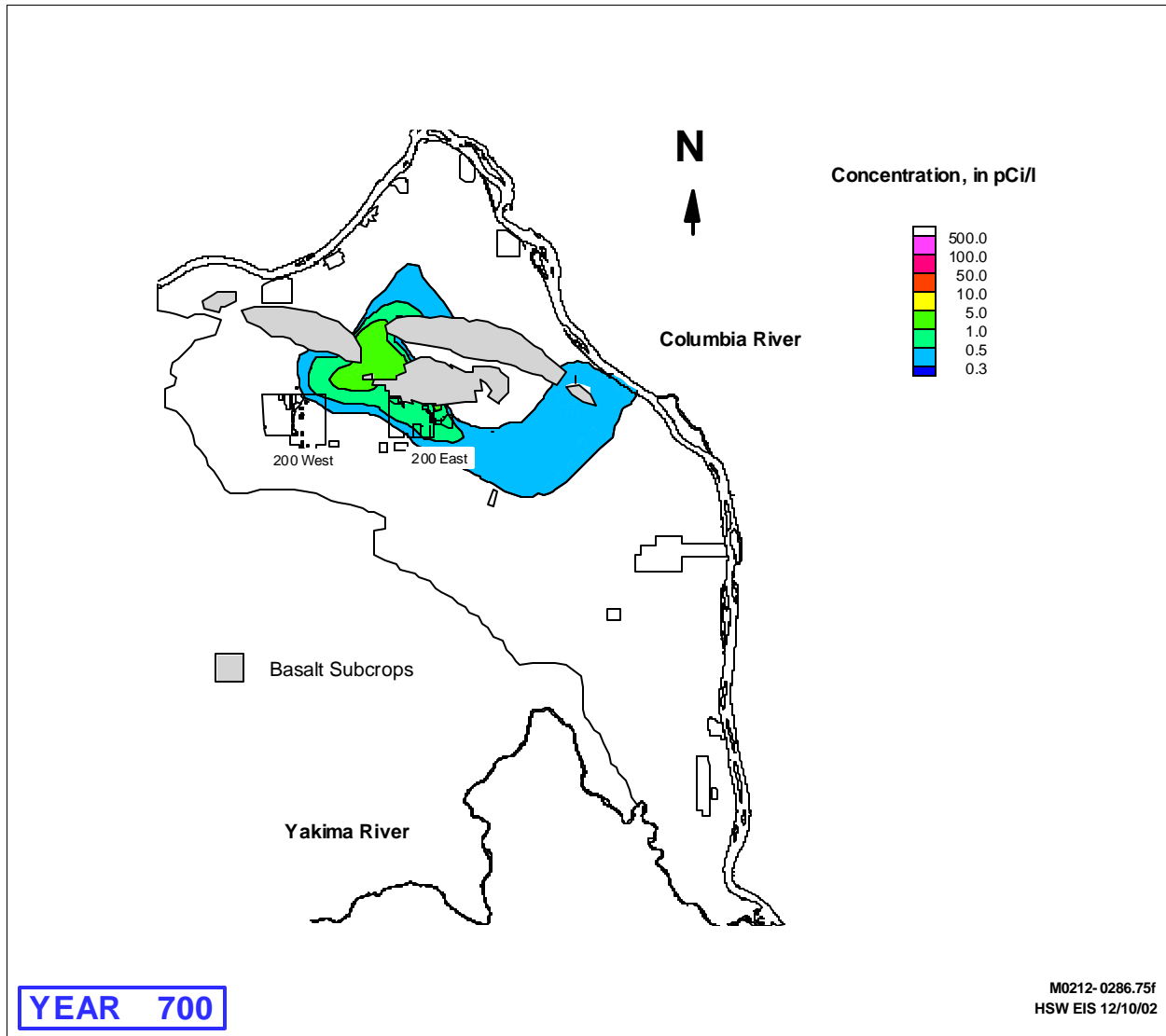
(a) These simulation results relate the effect of a known release (1 curie over a period of 10 years) of a hypothetical, long-lived contaminant in Mobility Class 1 to predicted concentrations at various points in the aquifer system. These results provide the basis for the groundwater transport component of the convolution approach described in Section G.1.2.



1  
2  
3  
4  
5  
6

**Figure G.14c.** Simulated Transport of a 10-Year Unit Release (1 Curie) of a Contaminant Representative of Mobility Class 1<sup>(a)</sup> from MLLW in the 200 West Area at 500 Years After Release Using a Groundwater Model with a Predominant Easterly Flow from the Central Plateau

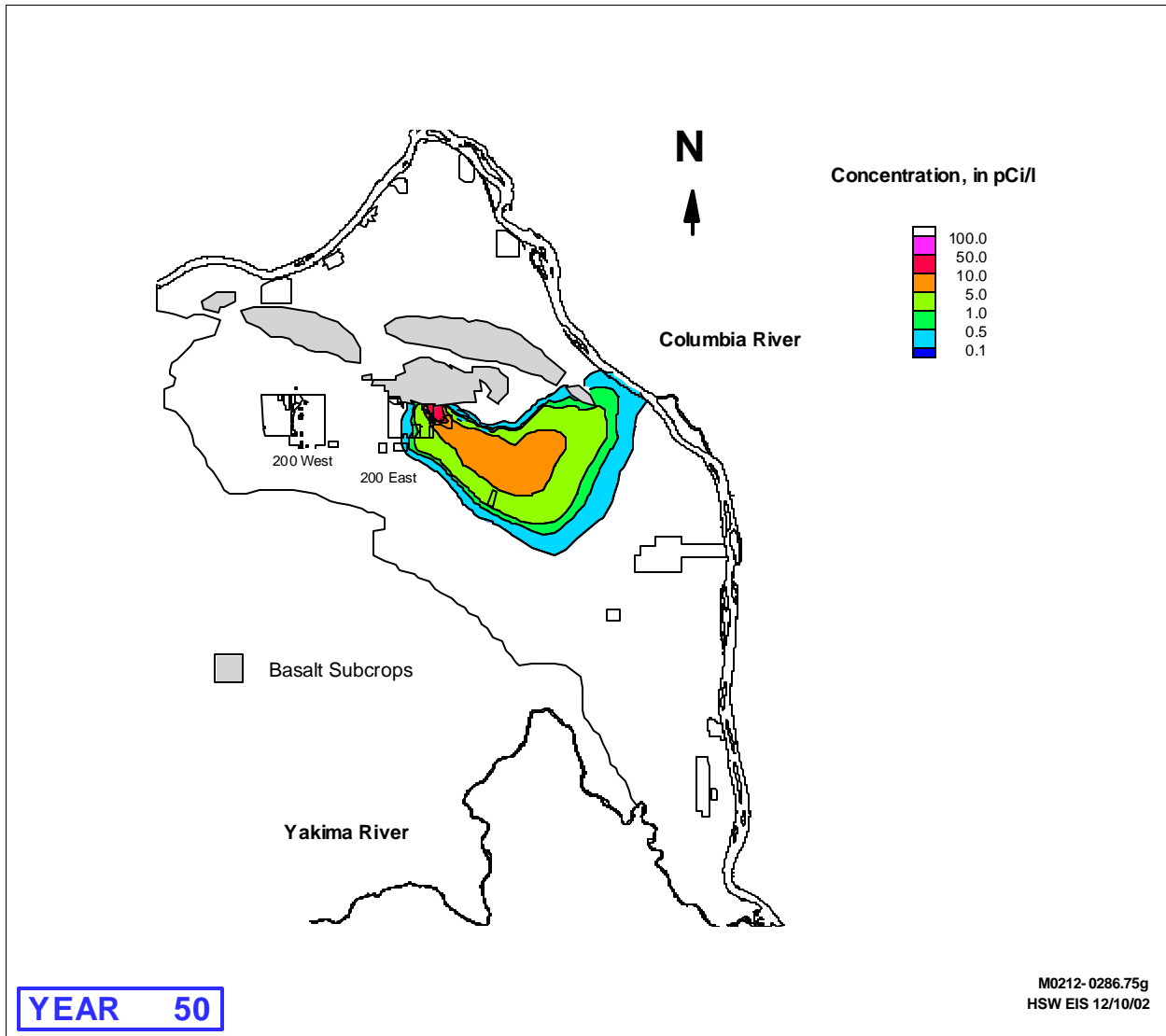
(a) These simulation results relate the effect of a known release (1 curie over a period of 10 years) of a hypothetical, long-lived contaminant in Mobility Class 1 to predicted concentrations at various points in the aquifer system. These results provide the basis for the groundwater transport component of the convolution approach described in Section G.1.2.



1  
2  
3  
4  
5  
6

**Figure G.14d.** Simulated Transport of a 10-Year Unit Release (1 Curie) of a Contaminant Representative of Mobility Class 1<sup>(a)</sup> from MLLW in the 200 West Area at 700 Years After Release Using a Groundwater Model with a Predominant Easterly Flow from the Central Plateau

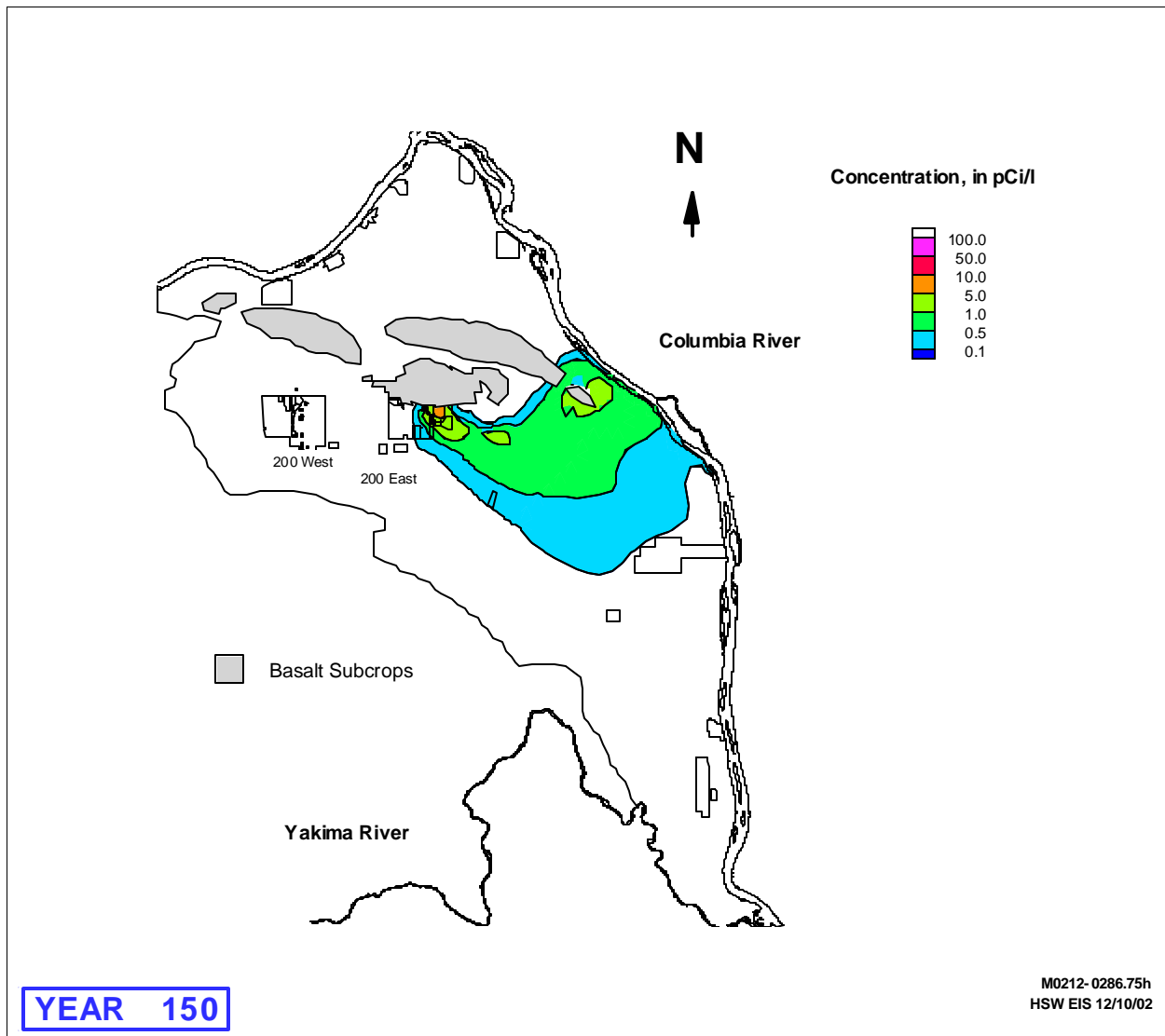
(a) These simulation results relate the effect of a known release (1 curie over a period of 10 years) of a hypothetical, long-lived contaminant in Mobility Class 1 to predicted concentrations at various points in the aquifer system. These results provide the basis for the groundwater transport component of the convolution approach described in Section G.1.2.



1  
2  
3  
4  
5  
6  
7

**Figure G.15a.** Simulated Transport of a 10-Year Unit Release (1 Curie) of of a Contaminant Representative of Mobility Class 1<sup>(a)</sup> from MLLW in the 200 East Area at 50 Years After Release Using a Groundwater Model with a Predominant Easterly Flow from the Central Plateau

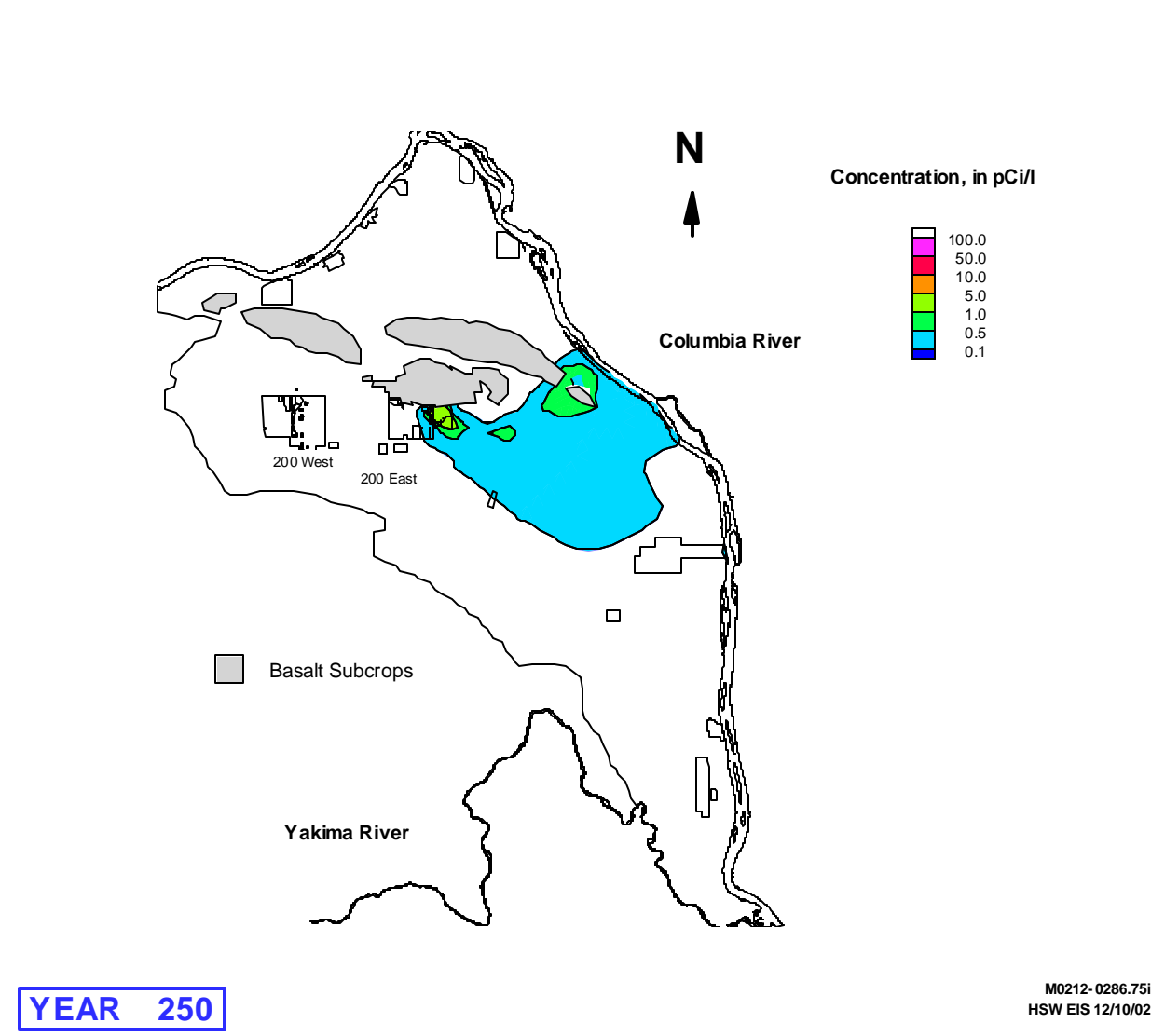
(a) These simulation results relate the effect of a known release (1 curie over a period of 10 years) of a hypothetical, long-lived contaminant in Mobility Class 1 to predicted concentrations at various points in the aquifer system. These results provide the basis for the groundwater transport component of the convolution approach described in Section G.1.2.



1  
2  
3  
4  
5  
6

**Figure G.15b.** Simulated Transport of a 10-Year Unit Release (1 Curie) of of a Contaminant Representative of Mobility Class 1<sup>(a)</sup> from MLLW in the 200 East Area at 150 Years After Release Using a Groundwater Model with a Predominant Easterly Flow from the Central Plateau

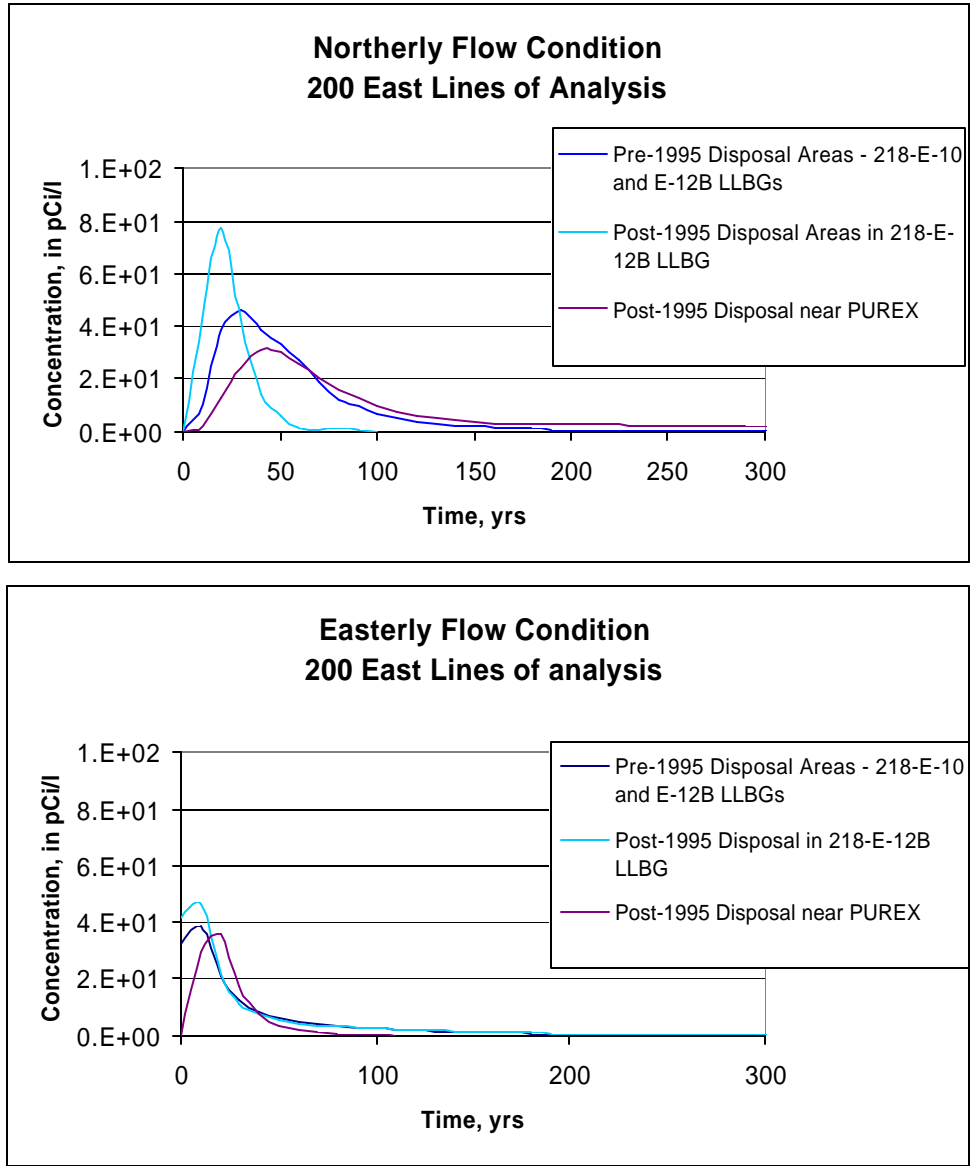
(a) These simulation results relate the effect of a known release (1 curie over a period of 10 years) of a hypothetical, long-lived contaminant in Mobility Class 1 to predicted concentrations at various points in the aquifer system. These results provide the basis for the groundwater transport component of the convolution approach described in Section G.1.2.



1  
2  
3  
4  
5  
6

**Figure G.15c.** Simulated Transport of a 10-Year Unit Release (1 Curie) of of a Contaminant Representative of Mobility Class 1<sup>(a)</sup> from MLLW in the 200 East Area at 250 Years After Release Using a Groundwater Model with a Predominant Easterly Flow from the Central Plateau

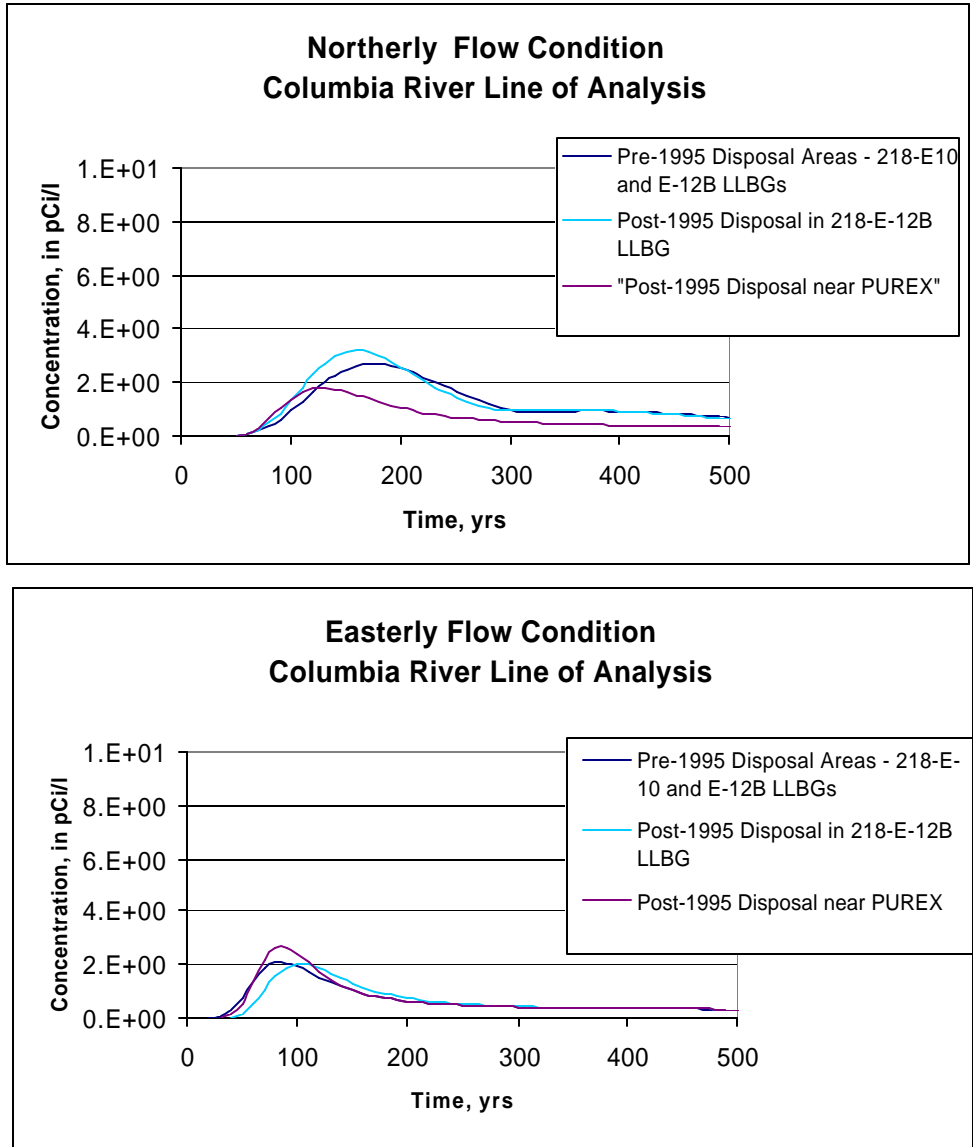
(a) These simulation results relate the effect of a known release (1 curie over a period of 10 years) of a hypothetical, long-lived contaminant in Mobility Class 1 to predicted concentrations at various points in the aquifer system. These results provide the basis for the groundwater transport component of the convolution approach described in Section G.1.2.



M0212-0286.76a  
HSW EIS 12/10/02

1  
2  
3  
4  
5

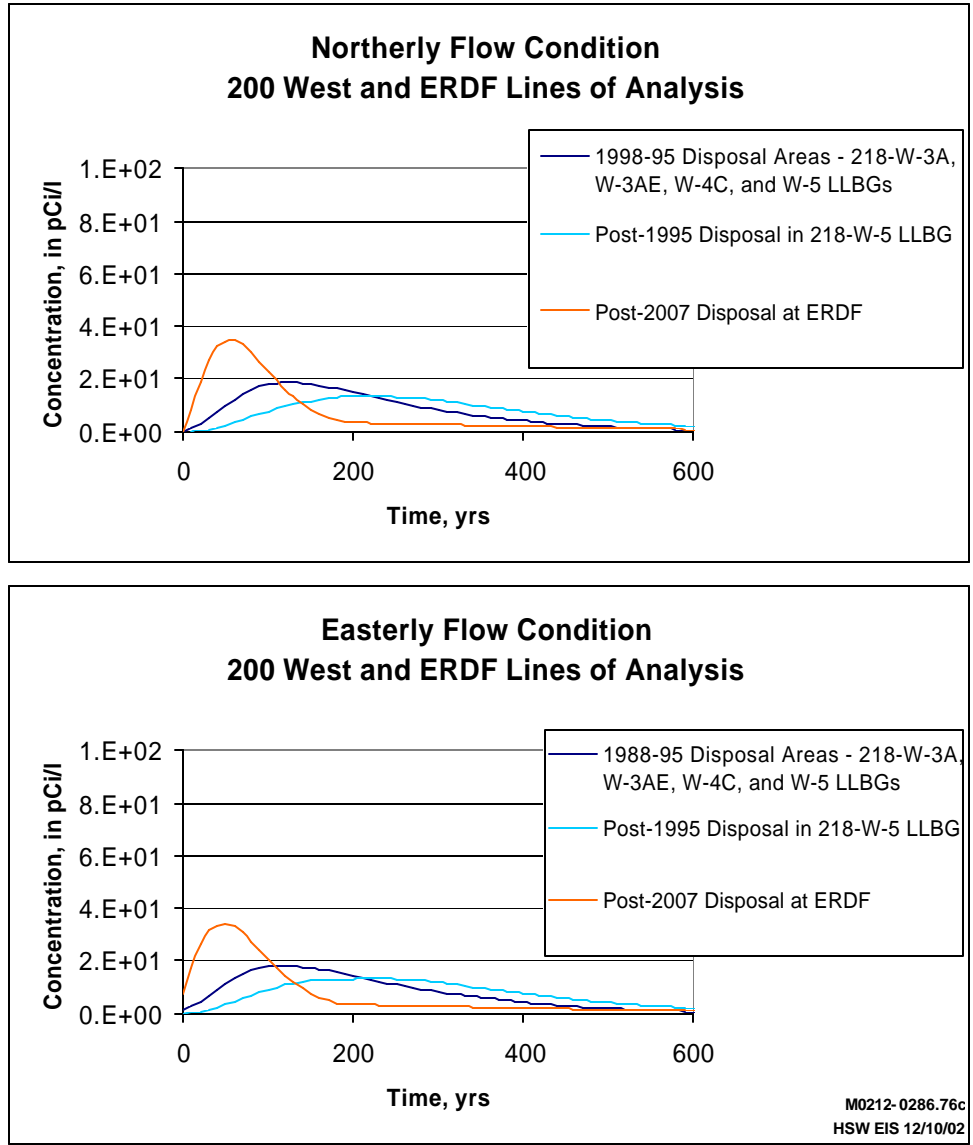
**Figure G.16a.** Comparison of Predicted Concentrations from Unit Releases from the 200 East Area at 200 East LOAs Using Groundwater Models with a Predominant Northerly and Easterly Flow from the Central Plateau



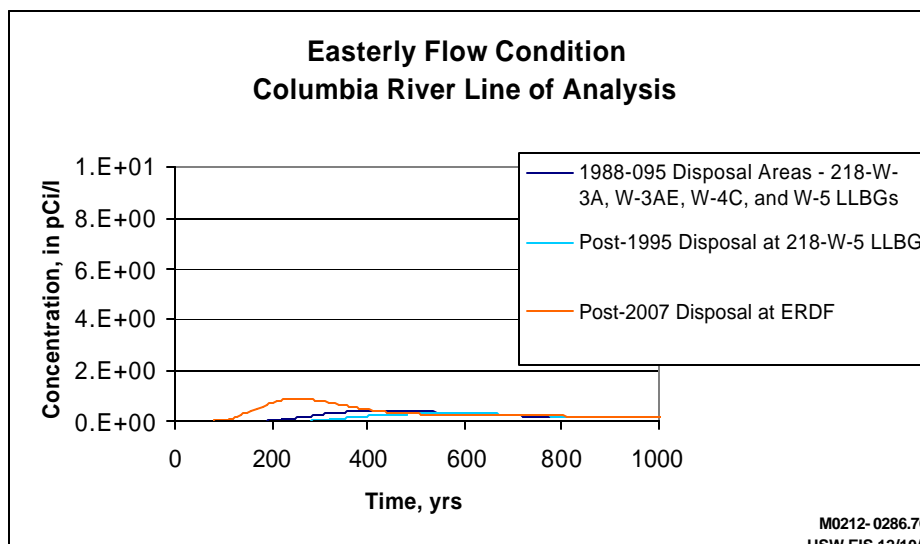
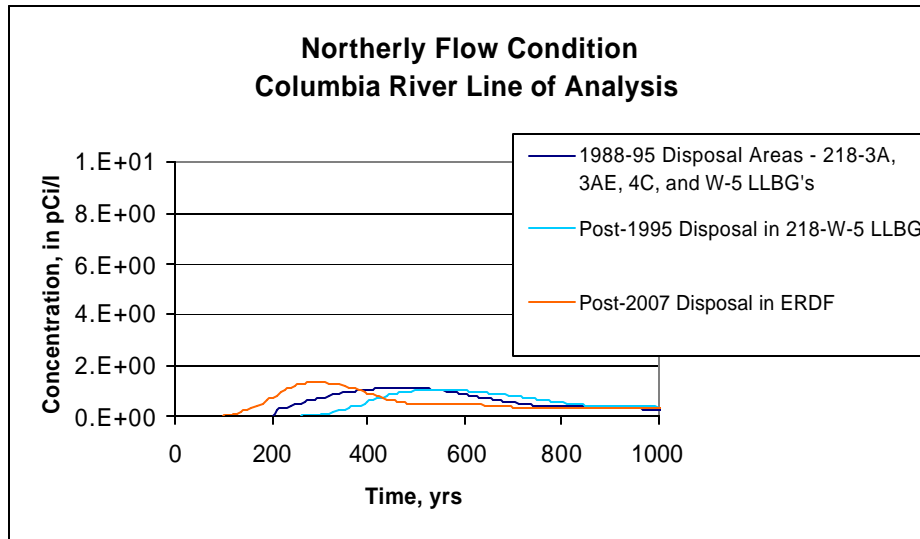
M0212-0286.76b  
 HSW EIS 12/10/02

1  
 2  
 3  
 4  
 5  
 6  
 7  
 8  
 9

**Figure G.16b.** Comparison of Predicted Concentrations from Unit Releases from the 200 East Area at Columbia River LOAs Using Groundwater Models with a Predominant Northerly and Easterly Flow from the Central Plateau



1  
 2 **Figure G.17a.** Comparison of Predicted Concentrations from Unit Releases from the 200 West Area at  
 3 the 200 West and ERDF LOAs Using Groundwater Models with a Predominant Northerly  
 4 and Easterly Flow from the Central Plateau



M0212-0286.76d  
HSW-EIS 12/4/02

1  
2 **Figure G.17b.** Comparison of Predicted Concentrations from Unit Releases from the 200 West Area at  
3 the Columbia River LOA Using Groundwater Models with a Predominant Northerly and  
4 Easterly Flow from the Central Plateau  
5

6 Results of these unit releases were evaluated to identify the maximum concentrations over time for  
7 use in the convolution approach along the LOAs down-gradient of the 200 East and West Areas and the  
8 ERDF HSW disposal areas (See Figure G.1) as appropriate for each alternative group. Because the  
9 location of different waste categories within each of the aggregate HSW disposal areas varies as specified  
10 for each alternative group, the locations of maximum concentration along the LOAs may not necessarily  
11 correspond to the same location for each waste category specified within and across alternative groups.  
12 This is particularly true for breakthrough curves developed for LOAs along the Columbia River where the  
13 location of maximum concentration varies in time as the simulated plumes migrate north to the  
14 Columbia River.